



Study of $B_c^+ \rightarrow \chi_c \pi^+$ decays

LHCb collaboration[†]

Abstract

A study of $B_c^+ \rightarrow \chi_c \pi^+$ decays is reported using proton-proton collision data, collected with the LHCb detector at centre-of-mass energies of 7, 8, and 13 TeV, corresponding to an integrated luminosity of 9 fb^{-1} . The decay $B_c^+ \rightarrow \chi_{c2} \pi^+$ is observed for the first time, with a significance exceeding seven standard deviations. The relative branching fraction with respect to the $B_c^+ \rightarrow J/\psi \pi^+$ decay is measured to be

$$\frac{\mathcal{B}_{B_c^+ \rightarrow \chi_{c2} \pi^+}}{\mathcal{B}_{B_c^+ \rightarrow J/\psi \pi^+}} = 0.37 \pm 0.06 \pm 0.02 \pm 0.01,$$

where the first uncertainty is statistical, the second is systematic, and the third is due to the knowledge of the $\chi_{c2} \rightarrow J/\psi \gamma$ branching fraction. No significant $B_c^+ \rightarrow \chi_{c1} \pi^+$ signal is observed and an upper limit for the relative branching fraction for the $B_c^+ \rightarrow \chi_{c1} \pi^+$ and $B_c^+ \rightarrow \chi_{c2} \pi^+$ decays of

$$\frac{\mathcal{B}_{B_c^+ \rightarrow \chi_{c1} \pi^+}}{\mathcal{B}_{B_c^+ \rightarrow \chi_{c2} \pi^+}} < 0.49$$

is set at the 90% confidence level.

Published in JHEP 02 (2024) 173

© 2024 CERN for the benefit of the LHCb collaboration. CC BY 4.0 licence.

[†]Authors are listed at the end of this paper.

1 Introduction

The B_c^+ meson, discovered in 1998 by the CDF collaboration [1,2] at the Tevatron collider, is the only known meson that contains two different heavy-flavour quarks, charm and beauty. The high b-quark production cross-section at the Large Hadron Collider (LHC) [3–8] enables the LHCb, ATLAS and CMS experiments to study in detail the production, decays and other properties of the B_c^+ meson [9–36]. The B_c^+ meson has a rich set of decay modes since either of the heavy quarks can decay while the other behaves as a spectator quark, or both quarks can annihilate via a virtual W^+ boson. Decays of the B_c^+ meson to charmonium and light hadrons can be described using the quantum chromodynamics (QCD) factorisation approach [37,38], which relies on the form factors of the $B_c^+ \rightarrow [c\bar{c}]W^+$ transition [39–43], and on the universal spectral function for the virtual W^+ boson fragmenting into light hadrons [44–46].

The decays of beauty hadrons into final states with P-wave charmonium, such as χ_{c1} and χ_{c2} mesons, have been extensively studied by the ARGUS [47], CLEO [48,49], BaBar [50–56], Belle [57–63], CDF [64] and LHCb [65–68] collaborations. In $B \rightarrow \chi_c K^{(*)}$ decays¹ a significant suppression of the tensor χ_{c2} state relative to the vector χ_{c1} state is observed in accordance with expectations from QCD factorisation [69]. In contrast, for decays of the beauty baryon Λ_b^0 , the $\Lambda_b^0 \rightarrow \chi_{c1} p K^-$ and $\Lambda_b^0 \rightarrow \chi_{c2} p K^-$ decay widths are found to be approximately the same [66]. A similar trend is observed for the $\Lambda_b^0 \rightarrow \chi_{c1} p \pi^-$ and $\Lambda_b^0 \rightarrow \chi_{c2} p \pi^-$ decays [68]. For decays of the B_c^+ meson the inverted pattern is expected with a relative suppression of the decays with the χ_{c1} meson in the final state [70–78]. However, the experimental information on the decays of the B_c^+ meson into P-wave charmonium states is very limited. Currently no decays of the B_c^+ meson into the χ_{c1} and χ_{c2} states are observed, and there is only evidence for the $B_c^+ \rightarrow (\chi_{c0} \rightarrow K^+ K^-) \pi^+$ decay with the scalar χ_{c0} meson in the final state [23]. Additional measurements are required to test the theory predictions and, in particular, to clarify the role of QCD factorisation in B_c^+ meson decays.

This paper reports a study of $B_c^+ \rightarrow \chi_c \pi^+$ decays using the radiative decays $\chi_c \rightarrow J/\psi \gamma$. A sample of $B_c^+ \rightarrow J/\psi \pi^+$ decays is used for the normalisation and a high-yield sample of $B^+ \rightarrow \chi_{c1} K^+$ decays is used to calibrate the detector resolution and mass scale. The analysis is based on proton-proton (pp) collision data, corresponding to an integrated luminosity of 9 fb^{-1} , collected with the LHCb detector at centre-of-mass energies of 7, 8, and 13 TeV.

2 Detector and simulation

The LHCb detector [79,80] is a single-arm forward spectrometer covering the pseudorapidity range $2 < \eta < 5$, designed for the study of particles containing b or c quarks. The detector includes a high-precision tracking system consisting of a silicon-strip vertex detector surrounding the pp interaction region [81], a large-area silicon-strip detector located upstream of a dipole magnet with a bending power of about 4 Tm, and three stations of silicon-strip detectors and straw drift tubes [82,83] placed downstream of the magnet. The tracking system provides a measurement of the momentum of charged particles with a relative uncertainty that varies from 0.5% at low momentum to 1.0% at 200 GeV/c.

¹In this paper the symbol χ_c denotes the χ_{c1} and χ_{c2} states together and inclusion of charge-conjugate decays is implied.

The momentum scale is calibrated using samples of $J/\psi \rightarrow \mu^+\mu^-$ and $B^+ \rightarrow J/\psi K^+$ decays collected concurrently with the data sample used for this analysis [84, 85]. The relative accuracy of this procedure is estimated to be 3×10^{-4} using samples of other fully reconstructed b hadrons, Υ and K_S^0 mesons. The minimum distance between a track and a primary pp-collision vertex (PV) [86, 87], the impact parameter, is measured with a resolution of $(15 + 29/p_T) \mu\text{m}$, where p_T is the component of the momentum transverse to the beam, in GeV/c . Different types of charged hadrons are distinguished using information from two ring-imaging Cherenkov detectors (RICH) [88]. Photons, electrons and hadrons are identified by a calorimeter system consisting of scintillating-pad and preshower detectors, an electromagnetic and a hadronic calorimeter. Muons are identified by a system composed of alternating layers of iron and multiwire proportional chambers [89].

The online event selection is performed by a trigger [90], which consists of a hardware stage, based on information from the calorimeter and muon systems, followed by a software stage, which performs a full event reconstruction. The hardware trigger selects muon candidates with high transverse momentum or dimuon candidates with a high value of the product of the transverse momenta of the two muons. In the software trigger, two oppositely-charged muons are required to form a good-quality vertex that is significantly displaced from any PV, and the mass of the $\mu^+\mu^-$ pair is required to exceed $2.7 \text{ GeV}/c^2$.

Simulated samples of $B_c^+ \rightarrow \chi_c \pi^+$, $B_c^+ \rightarrow J/\psi \pi^+$ and $B^+ \rightarrow \chi_c K^+$ decays are used to model the signal mass shapes, optimise the selection requirements and compute the efficiencies needed to determine the branching fraction ratios. The PYTHIA [91] generator with a specific LHCb configuration [92] is used to simulate pp collisions with B^+ meson production. For B_c^+ meson production the BCVEGPy generator [93–96] is used. It is based on the full perturbative QCD calculations at the lowest order α_s^4 via the dominant gluon-gluon fusion process $gg \rightarrow B_c^+ (B_c^{*+}) + \bar{c} + b$ and neglecting contributions from the quark pair annihilation $q\bar{q} \rightarrow B_c^+ (B_c^{*+}) + \bar{c} + b$ channel [97–101]. The generator is interfaced with the PYTHIA parton shower and hadronisation model. Decays of unstable particles are described by the EVTGEN package [102], in which final-state radiation is generated using PHOTOS [103].

The interaction of the generated particles with the detector, and its response, are implemented using the GEANT4 toolkit [104] as described in Ref. [105]. The transverse momentum and rapidity spectra of the B_c^+ mesons in simulated samples are adjusted to match those observed in a high-yield, low-background sample of reconstructed $B_c^+ \rightarrow J/\psi \pi^+$ decays. The detector response used for the identification of pions and kaons is sampled from the $D^{*+} \rightarrow (D^0 \rightarrow K^- \pi^+) \pi^+$ and $K_S^0 \rightarrow \pi^+ \pi^-$ control channels [88, 106]. To account for imperfections in the simulation of charged particle reconstruction, the track reconstruction efficiency determined from simulation is corrected using $J/\psi \rightarrow \mu^+\mu^-$ calibration samples [107]. Samples of $B^+ \rightarrow J/\psi (K^{*+} \rightarrow K^+ \pi^0)$ decays are used to correct the photon reconstruction efficiency in simulation [108–112].

3 Event selection

The signal $B_c^+ \rightarrow \chi_c \pi^+$ and control $B^+ \rightarrow \chi_c K^+$ candidates are reconstructed using $\chi_c \rightarrow J/\psi \gamma$ followed by $J/\psi \rightarrow \mu^+\mu^-$ decays. The dimuon final state of the J/ψ meson is used to reconstruct $B_c^+ \rightarrow J/\psi \pi^+$ candidates that are used as a normalisation channel. A loose preselection is applied, followed by a multivariate classifier based on a decision

tree with gradient boosting (BDTG) [113].

Muon, pion and kaon candidates are identified by combining information from the RICH, calorimeter and muon detectors. The candidates are required to have transverse momenta larger than 550 MeV/ c and 200 MeV/ c for muon and hadron candidates, respectively. Pions and kaons are required to have a momentum between 3.2 and 150 GeV/ c to ensure good performance of particle identification in the RICH detectors [88, 114]. To reduce combinatorial backgrounds from particles produced in pp interactions, only tracks that are inconsistent with originating from any PV are used.

Pairs of oppositely charged muons consistent with originating from a common vertex are combined to form $J/\psi \rightarrow \mu^+\mu^-$ candidates. The reconstructed mass of the $\mu^+\mu^-$ pair is required to be in the range $3.0 < m_{\mu^+\mu^-} < 3.2$ GeV/ c^2 . The position of the reconstructed dimuon vertex is required to be inconsistent with that of any reconstructed PV.

The $\chi_c \rightarrow J/\psi\gamma$ candidates are formed by combining the selected J/ψ candidates with photon candidates that have been reconstructed using clusters in the electromagnetic calorimeter. Only clusters that are not matched to the trajectory of a track extrapolated from the tracking system [115, 116] are used. The transverse energy of photon candidates is required to exceed 400 MeV. The χ_c candidates are selected in the $J/\psi\gamma$ mass region between 3.4 and 3.7 GeV/ c^2 , which covers both the $\chi_{c1} \rightarrow J/\psi\gamma$ and $\chi_{c2} \rightarrow J/\psi\gamma$ decays.

The selected χ_c and J/ψ candidates are combined with charged tracks identified as pions or kaons to form $B_c^+ \rightarrow \chi_c\pi^+$, $B^+ \rightarrow \chi_c K^+$ and $B_c^+ \rightarrow J/\psi\pi^+$ candidates. A kinematic fit [117] that constrains the three-track combination to form a common vertex is performed, in which the mass of the $\mu^+\mu^-$ combination is set equal to the known J/ψ mass [118] and the B candidate is constrained to originate from the associated PV.² A good fit quality is required to further suppress combinatorial background. The measured decay time of the selected candidate is required to be greater than 100 $\mu\text{m}/c$ and 150 $\mu\text{m}/c$ for the B_c^+ and B^+ candidates, respectively, to reduce the background from particles originating directly from the PV. To suppress the cross-feed from $B^+ \rightarrow J/\psi\pi^+$ decays, the mass of the $J/\psi\pi^+$ system for the reconstructed $B_c^+ \rightarrow \chi_c\pi^+$ candidates is required to be outside of the mass range $5.22 < m_{J/\psi\pi^+} < 5.35$ GeV/ c^2 .

To further suppress combinatorial background for the $B_c^+ \rightarrow \chi_c\pi^+$, $B_c^+ \rightarrow J/\psi\pi^+$ and $B^+ \rightarrow \chi_c K^+$ decays, three separate BDTG classifiers are used, each trained on the corresponding simulated samples. As a proxy for the background, the B_c^+ candidates from data with a mass between 6.4 and 6.6 GeV/ c^2 are used for the B_c^+ classifiers and B^+ candidates with a mass between 5.35 and 5.50 GeV/ c^2 are used for the B^+ classifier. The k -fold cross-validation technique [119] with $k = 13$ is used to avoid introducing a bias in the BDTG evaluation. The BDTG classifiers are trained using variables related to the reconstruction quality, decay time of B candidates, kinematics of particles in the final state and variables related to hadron (pion for B_c^+ candidates and kaon for B^+ candidates) identification [88, 114]. The requirement on the BDTG output is chosen to maximise the Punzi figure-of-merit $\varepsilon/(\alpha/2 + \sqrt{B})$ [120] for $B_c^+ \rightarrow \chi_c\pi^+$ decays and $S/\sqrt{S+B}$ for $B_c^+ \rightarrow J/\psi\pi^+$ and $B^+ \rightarrow \chi_c K^+$ decays, where ε is the signal efficiency in simulation for $B_c^+ \rightarrow \chi_c\pi^+$ decays, $\alpha = 5$ is the desired signal significance in units of standard deviations, B is the expected background yield within a narrow mass window centred at the known mass of the b-hadron [118], and the signal yields S are estimated

²Each B_c^+ or B^+ candidate is associated with the PV that yields the smallest χ_{IP}^2 , where χ_{IP}^2 is defined as the difference in the vertex-fit χ^2 of a given PV reconstructed with and without the particle under consideration.

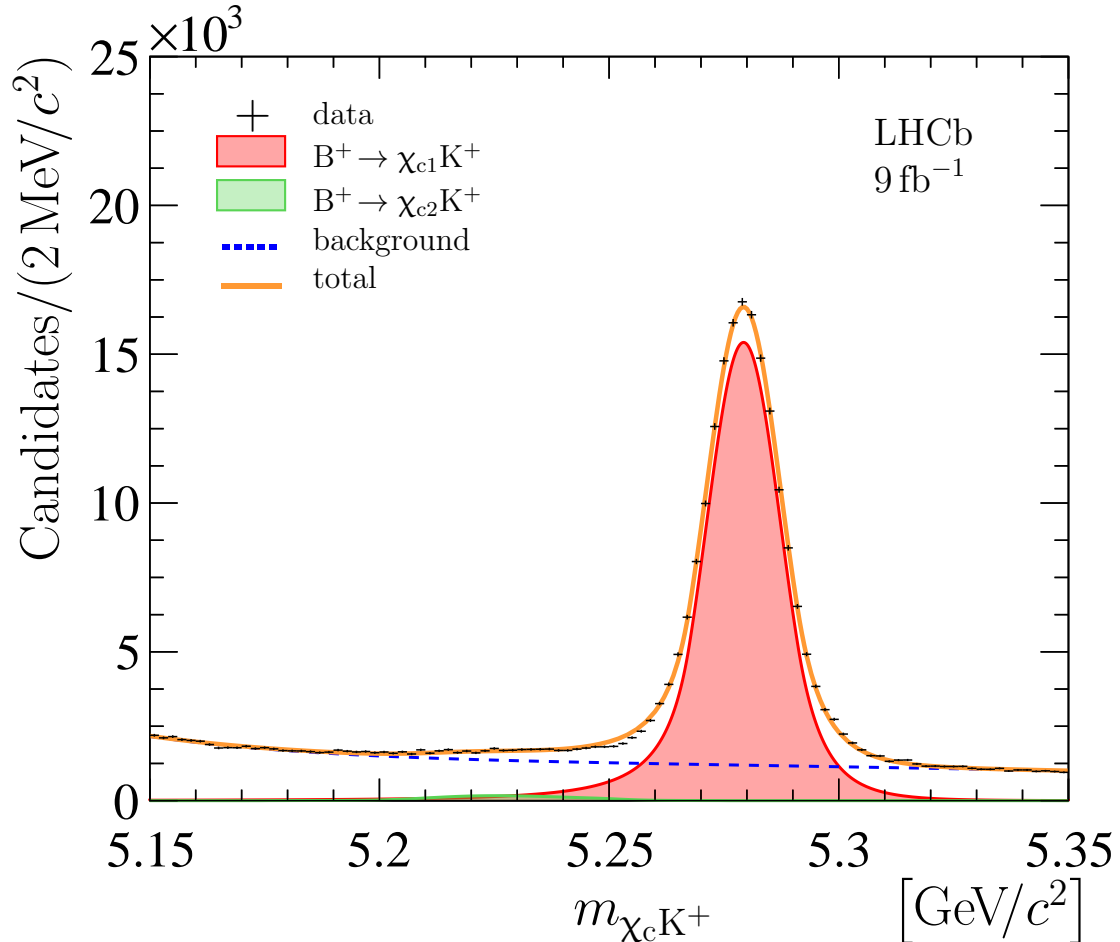


Figure 1: Mass distribution for selected $B^+ \rightarrow \chi_c K^+$ candidates with a χ_{c1} mass-constraint. The result of the fit, described in the text, is overlaid.

from simulated samples, normalised to the signal yields observed in data for a loose requirement on the BDTG output. After application of the BDTG requirement a small fraction of events, about 2.5% for the $B_c^+ \rightarrow \chi_c \pi^+$ and $B^+ \rightarrow \chi_c K^+$ candidates, and 0.5% for the $B_c^+ \rightarrow J/\psi \pi^+$ candidates in the signal region, contain multiple candidates. For each decay channel if two or more candidates are found in the same event, only one randomly chosen candidate is retained for further analysis.

To improve the B_c^+ and B^+ mass resolution, the mass of the B_c^+ and B^+ candidates is calculated using a kinematic fit [117], similar to the one described above, but with an additional constraint fixing the mass of the $J/\psi \gamma$ combination to the known χ_{c2} meson mass [118] for the $B_c^+ \rightarrow \chi_c \pi^+$ candidates, and to the known mass of the χ_{c1} meson [118] for the $B^+ \rightarrow \chi_c K^+$ candidates. The mass distributions for selected $B^+ \rightarrow \chi_c K^+$, $B_c^+ \rightarrow \chi_c \pi^+$ and $B_c^+ \rightarrow J/\psi \pi^+$ candidates are shown in Figs. 1, 2 and 3, respectively.

4 Signal yields

The yields for the $B^+ \rightarrow \chi_c K^+$, $B_c^+ \rightarrow \chi_c \pi^+$ and $B_c^+ \rightarrow J/\psi \pi^+$ decays are determined using extended unbinned maximum-likelihood fits. In this analysis, the detector resolution and a possible mass bias for the signal $B_c^+ \rightarrow \chi_c \pi^+$ channel are determined from the control

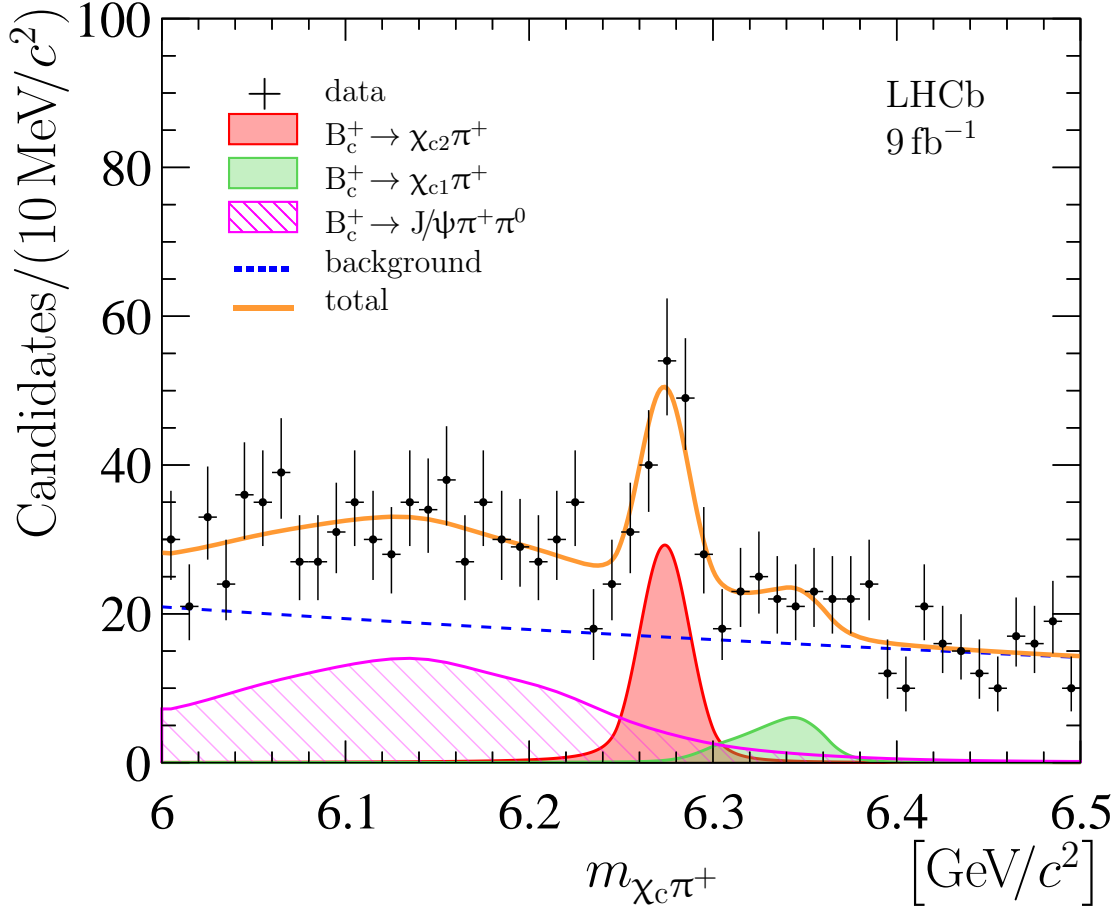


Figure 2: Mass distribution for selected $B_c^+ \rightarrow \chi_c \pi^+$ candidates with a χ_{c2} mass constraint. The result of the fit, described in the text, is overlaid.

channel $B^+ \rightarrow \chi_c K^+$, exploiting the similarity between the two final states.

The fit model for the $B^+ \rightarrow \chi_c K^+$ control channel consists of three components. The first component corresponds to the decay $B^+ \rightarrow \chi_{c1} K^+$, located close to the known mass of the B^+ meson, and is parameterised by a modified Gaussian function with power-law tails on both sides of the distribution [121, 122]. The second component corresponds to a small contribution from $B^+ \rightarrow \chi_{c2} K^+$ decays, and is parameterised by the sum of a Gaussian function and a modified Novosibirsk function [123]. Due to the mass difference between the χ_{c1} and χ_{c2} states [118, 124–126], the χ_{c1} -mass constraint used to evaluate the mass of the B^+ candidates shifts the position of this component toward lower masses. The third component corresponds to combinatorial background and is modelled by the product of an exponential function and a positive second-order polynomial function [127]. The shape parameters for the fit components describing the $B^+ \rightarrow \chi_{c1} K^+$ and $B^+ \rightarrow \chi_{c2} K^+$ decay contributions are taken from simulation and their uncertainties are propagated to the fit using a multivariate Gaussian constraint. The position and resolution parameters for the $B^+ \rightarrow \chi_{c1} K^+$ component are parameterised as

$$\mu_{B^+} = \delta m_{B^+} + m_{B^+}, \quad (1a)$$

$$\sigma_{B^+} = s_{B^+} \times \sigma_{B^+}^{\text{MC}}, \quad (1b)$$

where m_{B^+} is the known mass of the B^+ meson and $\sigma_{B^+}^{\text{MC}}$ is a resolution parameter

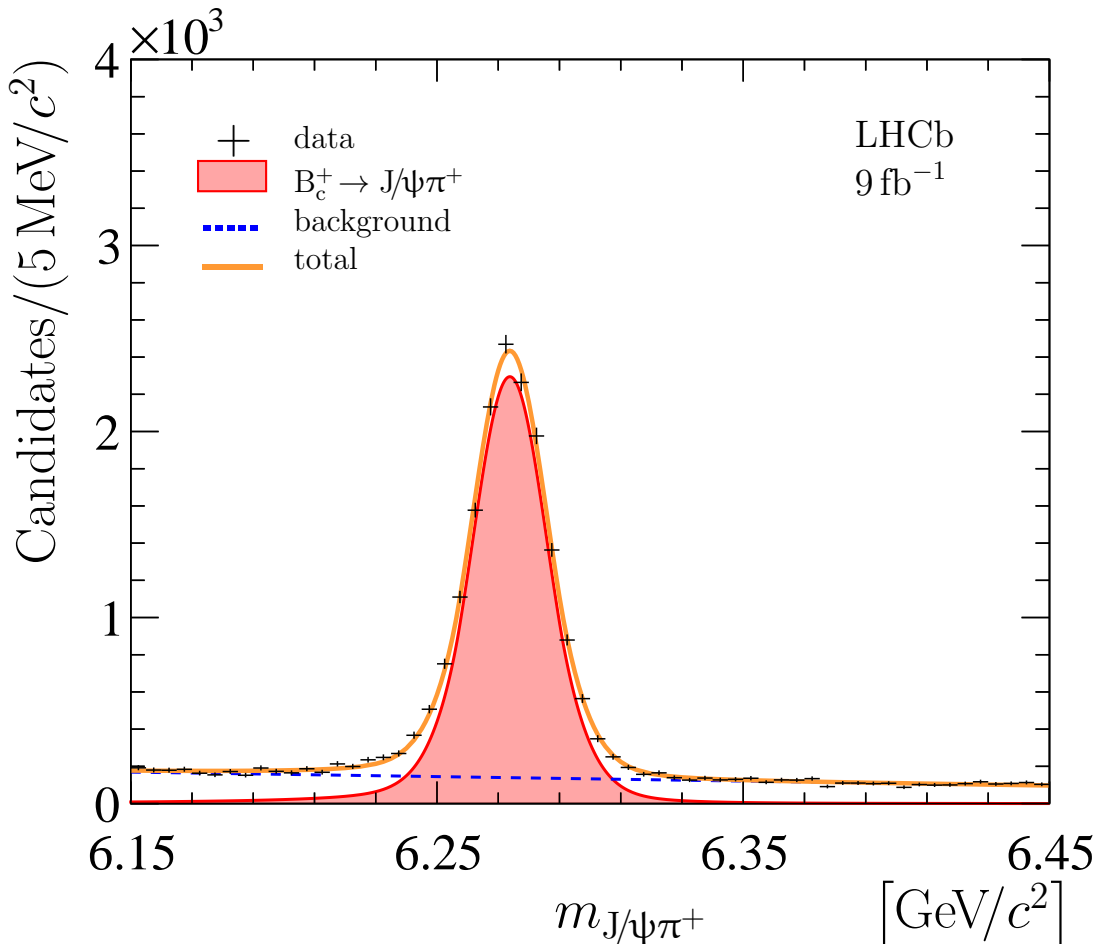


Figure 3: Mass distributions for selected $B_c^+ \rightarrow J/\psi\pi^+$ candidates. The result of the fit, described in the text, is overlaid.

obtained from simulation. The parameter δm_{B^+} accounts for a mass bias, while s_{B^+} describes potential differences between data and simulation for the resolution. The position parameters for the $B^+ \rightarrow \chi_{c1}K^+$ and $B^+ \rightarrow \chi_{c2}K^+$ components are allowed to vary in the fit, but their difference is constrained to the value obtained from simulation using a Gaussian constraint. The resulting fit is overlaid in Fig. 1, and the parameters of interest are listed in Table 1. The yield of the $B^+ \rightarrow \chi_{c2}K^+$ decay is found to be much smaller than that of the $B^+ \rightarrow \chi_{c1}K^+$ decay as seen in previous measurements [55, 59, 65] and in accordance with expectations from QCD factorisation. The obtained mass bias parameter δm_{B^+} and resolution scale parameter s_{B^+} are used for the determination of the signal yield for the $B_c^+ \rightarrow \chi_c\pi^+$ channel.

The fit model for the $B_c^+ \rightarrow \chi_c\pi^+$ channel consists of four components. The first component corresponds to the $B_c^+ \rightarrow \chi_{c2}\pi^+$ decay and is parameterised by a modified Gaussian function. This component is located close to the known mass of the B_c^+ meson. The second smaller component corresponds to the $B_c^+ \rightarrow \chi_{c1}\pi^+$ decay and is parameterised by the sum of a modified Gaussian and a modified Novosibirsk function. Due to the mass difference between the χ_{c1} and χ_{c2} states, and the χ_{c2} -mass constraint used to evaluate the mass of the B_c^+ candidate, the position of this component is shifted towards higher masses. The third component corresponds to the partially reconstructed $B_c^+ \rightarrow J/\psi\pi^+$ ($\pi^0 \rightarrow \gamma\gamma$) decay [128] where one photon is used in the misreconstructed

$\chi_c \rightarrow J/\psi\gamma$ candidate and the other is not reconstructed. The shape of this component is obtained from the simulation. Finally, the combinatorial background is parameterised by an exponential function. Similar to the $B^+ \rightarrow \chi_c K^+$ case above, the shape parameters for the fit components describing the $B_c^+ \rightarrow \chi_{c1}\pi^+$ and $B_c^+ \rightarrow \chi_{c2}\pi^+$ contributions and the difference between the positions of the mass peaks of the $B_c^+ \rightarrow \chi_{c1}\pi^+$ and $B_c^+ \rightarrow \chi_{c2}\pi^+$ contributions are taken from simulation. Their uncertainties are propagated to the fit using a multivariate Gaussian constraint. Similar to Eq. 1, the position and resolution parameters for the $B_c^+ \rightarrow \chi_{c2}\pi^+$ component are parameterised as

$$\mu_{B_c^+} = \delta m_{B^+} + m_{B_c^+}, \quad (2a)$$

$$\sigma_{B_c^+} = s_{B^+} \times \sigma_{B_c^+}^{\text{MC}}, \quad (2b)$$

where $m_{B_c^+}$ is the known mass of the B_c^+ meson [33] and $\sigma_{B_c^+}^{\text{MC}}$ is a resolution parameter obtained from simulation. The values of δm_{B^+} and s_{B^+} are defined in Eq. (1) and are taken from the fit to the $\chi_{c1}K^+$ mass spectrum above (see Table 1). Their uncertainties, as well as the uncertainty for the $m_{B_c^+}$ value, are propagated to the fit using Gaussian constraints. The yield of the $B_c^+ \rightarrow \chi_{c1}\pi^+$ signal component, $N_{B_c^+ \rightarrow \chi_{c1}\pi^+}$, is parameterised as

$$N_{B_c^+ \rightarrow \chi_{c1}\pi^+} \equiv N_{B_c^+ \rightarrow \chi_{c2}\pi^+} \times \mathcal{R}_{\chi_{c2}}^{\chi_{c1}} \times \varepsilon_{\chi_{c2}}^{\chi_{c1}} \times \frac{\mathcal{B}_{\chi_{c1} \rightarrow J/\psi\gamma}}{\mathcal{B}_{\chi_{c2} \rightarrow J/\psi\gamma}}, \quad (3a)$$

where $N_{B_c^+ \rightarrow \chi_{c2}\pi^+}$ is the yield of the $B_c^+ \rightarrow \chi_{c2}\pi^+$ signal component, $\mathcal{R}_{\chi_{c2}}^{\chi_{c1}}$ is a free parameter in the fit corresponding to the ratio of branching fractions for the $B_c^+ \rightarrow \chi_{c1}\pi^+$ and $B_c^+ \rightarrow \chi_{c2}\pi^+$ decays

$$\mathcal{R}_{\chi_{c2}}^{\chi_{c1}} \equiv \frac{\mathcal{B}_{B_c^+ \rightarrow \chi_{c1}\pi^+}}{\mathcal{B}_{B_c^+ \rightarrow \chi_{c2}\pi^+}}, \quad (3b)$$

$\mathcal{B}_{\chi_c \rightarrow J/\psi\gamma}$ are the branching fractions for the $\chi_c \rightarrow J/\psi\gamma$ decays [118], and $\varepsilon_{\chi_{c2}}^{\chi_{c1}}$ is the ratio of the total efficiencies for the $B_c^+ \rightarrow \chi_{c2}\pi^+$ and $B_c^+ \rightarrow \chi_{c1}\pi^+$ decays (see Sec. 5)

$$\varepsilon_{\chi_{c2}}^{\chi_{c1}} \equiv \frac{\varepsilon_{B_c^+ \rightarrow \chi_{c1}\pi^+}}{\varepsilon_{B_c^+ \rightarrow \chi_{c2}\pi^+}}. \quad (3c)$$

The uncertainties for the $\mathcal{B}_{\chi_c \rightarrow J/\psi\gamma}$ and $\varepsilon_{\chi_{c2}}^{\chi_{c1}}$ values including the systematic effects on the ratio of efficiencies, discussed in detail in Sec. 6, are accounted for in the fit via Gaussian constraints. The result of the fit is overlaid in Fig. 2. The parameters of interest,

Table 1: Parameters of interest from the fit to the $\chi_c K^+$ mass spectrum: the yields of the $B^+ \rightarrow \chi_{c1}K^+$ and $B^+ \rightarrow \chi_{c2}K^+$ decays, the B^+ mass bias parameter δm_{B^+} and the resolution scale factor s_{B^+} .

Parameter	Value
$N_{B^+ \rightarrow \chi_{c1}K^+}$	$[10^3] \quad 171.35 \pm 0.61$
$N_{B^+ \rightarrow \chi_{c2}K^+}$	$[10^3] \quad 3.28 \pm 0.40$
δm_{B^+}	$[\text{MeV}/c^2] \quad 0.07 \pm 0.12$
s_{B^+}	1.102 ± 0.004

namely the yield of the $B_c^+ \rightarrow \chi_{c2}\pi^+$ decays and the ratio of branching fractions $\mathcal{R}_{\chi_{c2}}^{\chi_{c1}}$, are found to be

$$\begin{aligned} N_{B_c^+ \rightarrow \chi_{c2}\pi^+} &= 108 \pm 16, \\ \mathcal{R}_{\chi_{c2}}^{\chi_{c1}} &= 0.24_{-0.11}^{+0.13}. \end{aligned}$$

The significance for the $B_c^+ \rightarrow \chi_{c2}\pi^+$ signal is estimated using Wilks' theorem [129] and found to be 8.1 standard deviations, corresponding to the first observation of the $B_c^+ \rightarrow \chi_{c2}\pi^+$ decay. On the contrary, the $B_c^+ \rightarrow \chi_{c1}\pi^+$ signal is found to be insignificant, exhibiting a hierarchy of branching fractions opposite to that in the $B^+ \rightarrow \chi_c K^+$ case, but in qualitative agreement with the theory expectation for the suppression of the χ_{c1} state in $B_c^+ \rightarrow \chi_c \pi^+$ decays [70–78]. Using the CL_s technique [130], where the p -values are calculated based on the asymptotic properties of the profile likelihood ratio [131], an upper limit of

$$\mathcal{R}_{\chi_{c2}}^{\chi_{c1}} < 0.41 \quad (4)$$

is found at 90% confidence level.

The fit model for the normalisation $B_c^+ \rightarrow J/\psi\pi^+$ channel consists of two components. The first component corresponds to the $B_c^+ \rightarrow J/\psi\pi^+$ decay and is parameterised by the sum of a modified Gaussian function and a Gaussian function with a common mean value. The second component describes the combinatorial background and is parameterised by a positive first-order polynomial function [127]. Similar to the $B^+ \rightarrow \chi_c K^+$ and $B_c^+ \rightarrow \chi_c \pi^+$ cases above, the shape parameters for the fit component describing the $B_c^+ \rightarrow J/\psi\pi^+$ contributions are taken from simulation and their uncertainties are propagated to the fit using a multivariate Gaussian constraint. The resolution parameter for the $B_c^+ \rightarrow J/\psi\pi^+$ component is parameterised as

$$\sigma_{B_c^+} = s_{B_c^+} \times \sigma_{B_c^+}^{\text{MC}}, \quad (5)$$

where $\sigma_{\text{MC}}^{B_c^+}$ is a resolution parameter obtained from simulation and the parameter $s_{B_c^+}$ accounts for a possible difference between data and simulation for the resolution parameter. The resulting fit is overlaid in Fig. 3. The parameters of interest, namely the yield of the $B_c^+ \rightarrow J/\psi\pi^+$ signal and the resolution scale parameter $s_{B_c^+}$, are found to be

$$\begin{aligned} N_{B_c^+ \rightarrow J/\psi\pi^+} &= (15.40 \pm 0.14) \times 10^3, \\ s_{B_c^+} &= 1.106 \pm 0.011. \end{aligned}$$

To validate the observed $B_c^+ \rightarrow \chi_{c2}\pi^+$ signal, several cross-checks are performed. The data are categorised according to the data-taking period, the polarity of the LHCb dipole magnet [132] and the charge of the B_c^+ candidates. Also, the χ_{c2} mass constraint, used for calculation of the mass of the B_c^+ candidates, is replaced by a χ_{c1} mass constraint. The results are found to be consistent among all samples and analysis techniques.

To confirm the $\chi_{c2} \rightarrow J/\psi\gamma$ signal within the observed $B_c^+ \rightarrow \chi_{c2}\pi^+$ signal, the background-subtracted $J/\psi\gamma$ mass spectrum is examined. For background subtraction, the *sPlot* technique [133] is used with the $\chi_c\pi^+$ mass as the discriminating variable. The background-subtracted $J/\psi\gamma$ spectrum is shown in Fig. 4 (left). The $\chi_{c1} \rightarrow J/\psi\gamma$ signal from the control sample of $B^+ \rightarrow \chi_{c1}K^+$ decays is used to examine the possible bias in the mass and mass resolution for the $J/\psi\gamma$ mass. The background-subtracted $J/\psi\gamma$ spectrum from

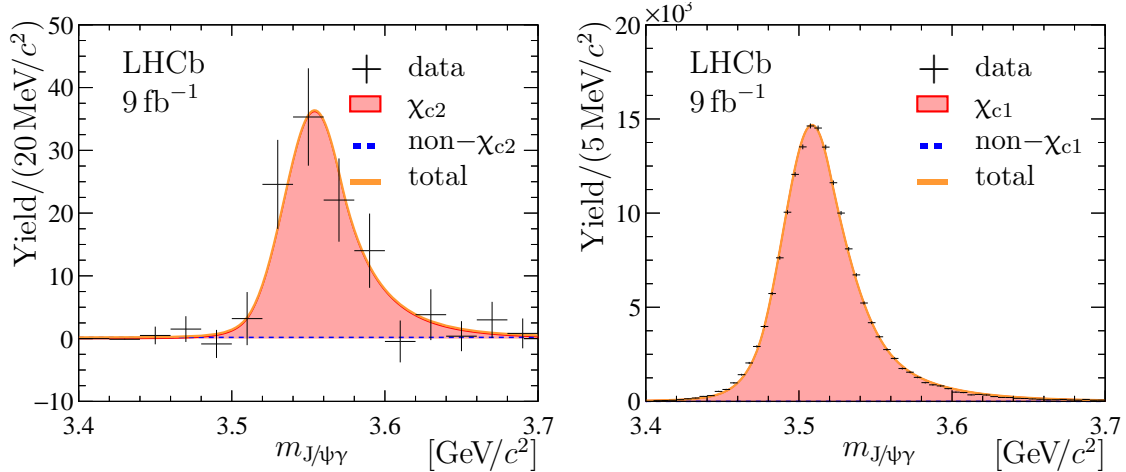


Figure 4: Background-subtracted $J/\psi\gamma$ mass distribution from (left) the $B_c^+ \rightarrow \chi_{c2}\pi^+$ decays and (right) $B^+ \rightarrow \chi_{c1}K^+$ decays. Projections of the fit, described in the text, are overlaid.

the $B^+ \rightarrow \chi_{c1}K^+$ decays is presented in Fig. 4 (right). Unbinned extended fits are performed to the $J/\psi\gamma$ distributions with a model consisting of two components. The first component corresponds to the $\chi_c \rightarrow J/\psi\gamma$ signal and is parameterised with a modified Gaussian function for the χ_{c2} state and the sum of a modified Gaussian function and a Gaussian function with a common mean value for the χ_{c1} state. The second component describes the $B_c^+ \rightarrow J/\psi\gamma\pi^+$ and $B^+ \rightarrow J/\psi\gamma K^+$ decays without intermediate χ_{c2} and χ_{c1} mesons and is parameterised with a constant. Similar to the fits described above, the shape parameters for the χ_c components are taken from simulation and their uncertainties are propagated to the fits using a multivariate Gaussian constraint. Similar to Eqs. (1) and (2) the position and resolution parameters for each χ_c component in the fits are parameterised as

$$\mu_{\chi_c} = \delta m_{\chi_{c1}} + m_{\chi_c}, \quad (6a)$$

$$\sigma_{\chi_c} = s_{\chi_{c1}} \times \sigma_{\chi_c}^{\text{MC}}, \quad (6b)$$

where m_{χ_c} stands for the known mass of the corresponding χ_c state and $\sigma_{\text{MC}}^{\chi_c}$ denotes the corresponding resolution parameter obtained from simulation. The mass bias parameter $\delta m_{\chi_{c1}}$ and resolution scale parameter $s_{\chi_{c1}}$, determined from the fit to the $J/\psi\gamma$ mass spectrum from the control $B^+ \rightarrow \chi_{c1}K^+$ channel, are $\delta m_{\chi_{c1}} = -2.09 \pm 0.09 \text{ MeV}/c^2$ and $s_{\chi_{c1}} = 1.027 \pm 0.004$. These values are used in the fit to the $J/\psi\gamma$ mass spectrum for the signal $B_c^+ \rightarrow \chi_{c2}\pi^+$ channel and their uncertainties are included using Gaussian constraints. The results of the fits to both $J/\psi\gamma$ mass spectra are overlaid in Fig. 4. For both $B^+ \rightarrow \chi_{c1}K^+$ and $B_c^+ \rightarrow \chi_{c2}\pi^+$ decays a good description of data is achieved without contributions from the non- χ_c components. This proves the observed $B_c^+ \rightarrow (J/\psi\gamma)\pi^+$ signal proceeds via the intermediate $\chi_{c2} \rightarrow J/\psi\gamma$ decay.

5 Efficiency and ratio of branching fractions

For each channel, the efficiency is defined as the product of the detector acceptance, reconstruction, selection and trigger efficiencies, where each subsequent efficiency is defined with respect to the previous one. Each of the efficiencies is calculated using the simulation samples described in Sec. 2. The ratio of efficiencies for the $B_c^+ \rightarrow \chi_{c1}\pi^+$

and $B_c^+ \rightarrow \chi_{c2}\pi^+$ channels, $\varepsilon_{\chi_{c2}}^{\chi_{c1}}$, defined in Eq. (3c), and the ratio of efficiencies for the $B_c^+ \rightarrow \chi_{c2}\pi^+$ and $B_c^+ \rightarrow J/\psi\pi^+$ channels, $\varepsilon_{J/\psi}^{\chi_{c2}}$, are found to be

$$\varepsilon_{\chi_{c2}}^{\chi_{c1}} = 0.763 \pm 0.003, \quad (7a)$$

$$\varepsilon_{J/\psi}^{\chi_{c2}} = (9.84 \pm 0.03) \times 10^{-2}, \quad (7b)$$

where the uncertainties are due to the size of simulated samples.

The ratio of branching fractions for the $B_c^+ \rightarrow \chi_{c2}\pi^+$ and $B_c^+ \rightarrow J/\psi\pi^+$ decays is calculated as

$$\mathcal{R}_{J/\psi}^{\chi_{c2}} \equiv \frac{\mathcal{B}_{B_c^+ \rightarrow \chi_{c2}\pi^+}}{\mathcal{B}_{B_c^+ \rightarrow J/\psi\pi^+}} = \frac{N_{B_c^+ \rightarrow \chi_{c2}\pi^+}}{N_{B_c^+ \rightarrow J/\psi\pi^+}} \times \frac{1}{\varepsilon_{J/\psi}^{\chi_{c2}}} \times \frac{1}{\mathcal{B}_{\chi_{c2} \rightarrow J/\psi\gamma}}, \quad (8)$$

where the signal yields N are obtained in Sec. 4, $\varepsilon_{J/\psi}^{\chi_{c2}}$ is the efficiency ratio from Eq. (7b) and $\mathcal{B}_{\chi_{c2} \rightarrow J/\psi\gamma}$ is the known branching fraction of the $\chi_{c2} \rightarrow J/\psi\gamma$ decay [118]. The ratio of branching fractions is found to be

$$\mathcal{R}_{J/\psi}^{\chi_{c2}} = 0.37 \pm 0.06,$$

where the uncertainty is statistical only. Systematic uncertainties are discussed in the following section.

6 Systematic uncertainties

The decay channels under study have similar kinematics and topologies; therefore, many sources of systematic uncertainty cancel in the branching fraction ratios. The remaining contributions to the systematic uncertainty are summarised in Table 2 and discussed below.

An important source of systematic uncertainty is the imperfect knowledge of the shapes of the signal and background components used in the fits. To estimate this, several alternative shapes are tested. For the $B_c^+ \rightarrow \chi_{c2}\pi^+$ and $B_c^+ \rightarrow J/\psi\pi^+$ signal shapes two alternative models are tested:

- the sum of a generalised Student's t -distribution [134] and a Gaussian function;
- the sum of a modified Apollonios function [135] and a Gaussian function.

For the $B_c^+ \rightarrow \chi_{c1}\pi^+$ signal shape two alternative models are probed:

- the sum of a generalised Student's t -distribution and a modified Novosibirsk function [123];
- the sum of a modified Apollonios function and a modified Novosibirsk function.

For the background components, positive convex decreasing polynomial functions of the second and third-order are used as alternative background shapes for the fit to the $\chi_c\pi^+$ mass spectrum. For the fit to the $J/\psi\pi^+$ mass spectrum the product of an exponential function and a positive first-order polynomial function as well as a positive second-order polynomial function are tested. The systematic uncertainty related to the fit model is estimated using pseudoexperiments produced with the baseline fit model and fit with sets of the alternative models. The maximal deviations in the ratios of the signal

Table 2: Relative systematic uncertainties (in %) for the ratio of branching fractions $\mathcal{R}_{J/\psi}^{\chi_{c2}}$ and the ratio of efficiencies for the $B_c^+ \rightarrow \chi_{c1}\pi^+$ and $B_c^+ \rightarrow \chi_{c2}\pi^+$ decays. The total uncertainty is the quadratic sum of individual contributions.

Source	$\mathcal{R}_{J/\psi}^{\chi_{c2}}$	$\varepsilon_{\chi_{c2}}^{\chi_{c1}}$
Fit model		
Signal shape	0.3	—
Background shape	0.7	—
Multiple candidates exclusion	2.0	—
B_c^+ production spectra	0.3	0.1
Track reconstruction	< 0.1	< 0.1
Photon reconstruction	3.0	—
Pion identification	0.5	0.6
Trigger efficiency	1.1	1.1
Data-simulation difference	2.1	—
Size of simulated sample	0.3	0.4
Total	4.4	1.3

yields for the $B_c^+ \rightarrow \chi_{c2}\pi^+$ and $B_c^+ \rightarrow J/\psi\pi^+$ decays with respect to the baseline models do not exceed 0.3% for the alternative signal models and 0.7% for the alternative background models. These values are taken as systematic uncertainties for the ratio $\mathcal{R}_{J/\psi}^{\chi_{c2}}$.

In the analysis, multiple candidates are randomly excluded. To estimate the systematic effect due to the exclusion procedure the analysis is repeated 300 times with different sets of candidates randomly removed. The variation of the relative signal yield between $B_c^+ \rightarrow \chi_{c2}\pi^+$ and $B_c^+ \rightarrow J/\psi\pi^+$ channels is found to be 2.0% and this value is assigned as the corresponding systematic uncertainty.

An important systematic uncertainty arises from differences between data and simulation. The transverse momentum and rapidity spectra of the B_c^+ mesons in the simulated samples are adjusted to match those observed in a high-yield, low-background sample of $B_c^+ \rightarrow J/\psi\pi^+$ decays. The finite size of this sample causes uncertainty in the obtained production spectra of the B_c^+ mesons. The associated systematic uncertainty in the efficiency ratios is estimated using the variation of the B_c^+ kinematic spectra within their uncertainties. The induced variations for the ratio $\mathcal{R}_{J/\psi}^{\chi_{c2}}$ and for the efficiency ratio $\varepsilon_{\chi_{c2}}^{\chi_{c1}}$ are found to be 0.3% and 0.1%, respectively. These values are taken as corresponding systematic uncertainties.

Due to the slightly different kinematic distributions of the final-state particles there are residual differences in the reconstruction efficiency of charged-particle tracks that do not cancel completely in the efficiency ratios. The track-finding efficiency obtained from simulated samples is corrected using calibration channels [107]. The uncertainties related to the efficiency correction factors are propagated to the ratios of the total efficiencies using pseudoexperiments and found to be smaller than 0.1% both for the ratio $\mathcal{R}_{J/\psi}^{\chi_{c2}}$ and for the efficiency ratio $\varepsilon_{\chi_{c2}}^{\chi_{c1}}$. Differences in the photon reconstruction efficiencies between data and simulation are studied using a large sample of $B^+ \rightarrow J/\psi (K^{*+} \rightarrow K^+\pi^0)$ decays [110–112]. The uncertainty due to the finite size of the sample is propagated to

the ratio of the total efficiencies using pseudoexperiments and is found to be less than 0.1%. The additional uncertainty due to the imprecise knowledge of the ratio of branching fractions for the $B^+ \rightarrow J/\psi K^{*+}$ and $B^+ \rightarrow J/\psi K^+$ decays [118] is 3.0%. The squared sum of these uncertainties is taken as a systematic uncertainty for the ratio $\mathcal{R}_{J/\psi}^{\chi_{c2}}$ related to the photon reconstruction. The corresponding systematic uncertainty for the efficiency ratio $\varepsilon_{\chi_{c2}}^{\chi_{c1}}$ is found to be negligible.

The modelling of the pion identification in the simulation is improved by sampling the corresponding distributions in the $D^{*+} \rightarrow (D^0 \rightarrow K^- \pi^+) \pi^+$ and $K_S^0 \rightarrow \pi^+ \pi^-$ control channels [88, 106]. The systematic uncertainty obtained through this procedure arises from the kernel shape used in the estimation of the probability density distributions. An alternative response is estimated using a different kernel estimation with a changed shape and the efficiency models are regenerated [136, 137]. The difference between the two estimates for the efficiency ratios is taken as the systematic uncertainty related to pion identification and is found to be 0.5% and 0.6% for the ratio $\mathcal{R}_{J/\psi}^{\chi_{c2}}$ and for the efficiency ratio $\varepsilon_{\chi_{c2}}^{\chi_{c1}}$, respectively.

Large samples of $B^+ \rightarrow J/\psi K^+$ and $B^+ \rightarrow \psi(2S)K^+$ decays [138] are used to estimate the systematic uncertainty related to the trigger efficiency. A conservative estimate of 1.1% for the relative difference between data and simulation is taken as the corresponding systematic uncertainty [138].

Discrepancies in reconstructed quantities between the simulated samples and data, due to effects other than those described above, are studied by varying the BDTG selection criteria for the normalisation decay $B_c^+ \rightarrow J/\psi \pi^+$ over its full range and repeating the fit. The observed maximal difference between the efficiency estimated using data and simulation does not exceed 2.1%. This value is taken as a corresponding systematic uncertainty for the ratio $\mathcal{R}_{J/\psi}^{\chi_{c2}}$. The corresponding systematic uncertainty for the efficiency ratio $\varepsilon_{\chi_{c2}}^{\chi_{c1}}$ is considered to be negligible due to the very similar kinematics of the corresponding decay channels.

The systematic uncertainty due to the finite size of the simulated samples, used to calculate the efficiency ratios from Eqs. (7), is found to be 0.3% and 0.4% for the ratio $\mathcal{R}_{J/\psi}^{\chi_{c2}}$ and for the efficiency ratio $\varepsilon_{\chi_{c2}}^{\chi_{c1}}$, respectively. The total systematic uncertainty is estimated as the sum in quadrature of the individual contributions.

For each choice of an alternative fit model and for each pseudoexperiment with random removal of multiple candidates, the statistical significance for the $B_c^+ \rightarrow \chi_{c2} \pi^+$ decay is recalculated using Wilks' theorem [129]. The smallest significance of 7.6 standard deviations is taken as the overall significance of the signal, including systematic uncertainties.

The systematic uncertainty for the efficiency ratio $\varepsilon_{\chi_{c2}}^{\chi_{c1}}$, discussed above, is included in the fit model via a Gaussian constraint. Therefore the upper limit for the $\mathcal{R}_{\chi_{c2}}^{\chi_{c1}}$ ratio from Eq. (4) already accounts for the corresponding systematic uncertainty. The remaining uncertainties are related to the fit model and the exclusion of multiple candidates. To account for these, the upper limit is recalculated for each fit with the alternative models and for each pseudoexperiment with random removal of multiple candidates and the maximal obtained value of

$$\mathcal{R}_{\chi_{c2}}^{\chi_{c1}} < 0.49 \text{ at } 90\% \text{ CL}$$

is conservatively taken as the upper limit including systematic uncertainties.

7 Results and conclusions

The decay modes $B_c^+ \rightarrow \chi_c \pi^+$ are studied using proton-proton collision data, corresponding to an integrated luminosity of 9 fb^{-1} , collected with the LHCb detector at centre-of-mass energies of 7, 8, and 13 TeV. The first observation of the decay $B_c^+ \rightarrow \chi_{c2} \pi^+$, with a significance of 7.6 standard deviations, is reported. Using the $B_c^+ \rightarrow J/\psi \pi^+$ decay as a normalisation channel, and the known value of the branching fraction for the $\chi_{c2} \rightarrow J/\psi \gamma$ decay of $(19.0 \pm 0.5)\%$ [118], the ratio of the branching fractions is measured to be

$$\frac{\mathcal{B}_{B_c^+ \rightarrow \chi_{c2} \pi^+}}{\mathcal{B}_{B_c^+ \rightarrow J/\psi \pi^+}} = 0.37 \pm 0.06 \pm 0.02 \pm 0.01,$$

where the first uncertainty is statistical, the second is systematic and the third is due to knowledge of the $\chi_{c2} \rightarrow J/\psi \gamma$ branching fraction [118]. The measured value is compatible with predictions from Refs. [72] and [73].

No significant $B_c^+ \rightarrow \chi_{c1} \pi^+$ signal is observed and the upper limit on the relative branching fraction between the $B_c^+ \rightarrow \chi_{c1} \pi^+$ and $B_c^+ \rightarrow \chi_{c2} \pi^+$ decays is found to be

$$\frac{\mathcal{B}_{B_c^+ \rightarrow \chi_{c1} \pi^+}}{\mathcal{B}_{B_c^+ \rightarrow \chi_{c2} \pi^+}} < 0.49 \text{ at } 90\% \text{ CL}.$$

The comparison of this upper limit with theoretical predictions, reported in Refs. [70–77] is shown in Fig. 5. The upper limit obtained is in agreement with all but one prediction and disfavors the calculation from the relativistic quark model [71].

LHCb 2023 (90% CL)

C.-H. Chang <i>et al.</i>	[70]
D. Ebert <i>et al.</i>	[71]
E. Hernández <i>et al.</i>	[72]
M. A. Ivanov <i>et al.</i>	[73]
V. V. Kiselev <i>et al.</i>	[74]
Z. Rui	[75]
Z.-h. Wang <i>et al.</i>	[76]
R. Zhu	[77]

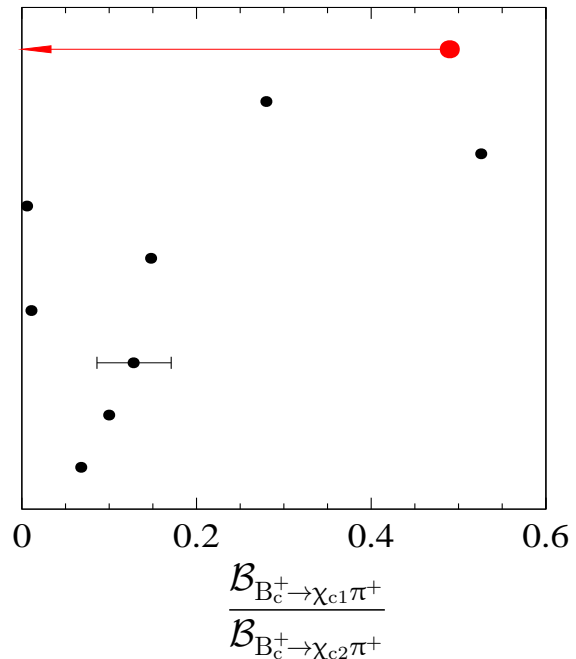


Figure 5: Comparison of upper limit on the branching fraction ratio between $B_c^+ \rightarrow \chi_{c1} \pi^+$ and $B_c^+ \rightarrow \chi_{c2} \pi^+$ decays set in this analysis with theoretical predictions.

Acknowledgements

We thank A.K. Likhoded, X. Liu and A.V. Luchinsky for the interesting and stimulating discussions on the physics of the B_c^+ mesons and their decays. We express our gratitude to our colleagues in the CERN accelerator departments for the excellent performance of the LHC. We thank the technical and administrative staff at the LHCb institutes. We acknowledge support from CERN and from the national agencies: CAPES, CNPq, FAPERJ and FINEP (Brazil); MOST and NSFC (China); CNRS/IN2P3 (France); BMBF, DFG and MPG (Germany); INFN (Italy); NWO (Netherlands); MNiSW and NCN (Poland); MCID/IFA (Romania); MICINN (Spain); SNSF and SER (Switzerland); NASU (Ukraine); STFC (United Kingdom); DOE NP and NSF (USA). We acknowledge the computing resources that are provided by CERN, IN2P3 (France), KIT and DESY (Germany), INFN (Italy), SURF (Netherlands), PIC (Spain), GridPP (United Kingdom), CSCS (Switzerland), IFIN-HH (Romania), CBPF (Brazil), and Polish WLCG (Poland). We are indebted to the communities behind the multiple open-source software packages on which we depend. Individual groups or members have received support from ARC and ARDC (Australia); Key Research Program of Frontier Sciences of CAS, CAS PIFI, CAS CCEPP, Fundamental Research Funds for the Central Universities, and Sci. & Tech. Program of Guangzhou (China); Minciencias (Colombia); EPLANET, Marie Skłodowska-Curie Actions, ERC and NextGenerationEU (European Union); A*MIDEX, ANR, IPhU and Labex P2IO, and Région Auvergne-Rhône-Alpes (France); AvH Foundation (Germany); ICSC (Italy); GVA, XuntaGal, GENCAT, Inditex, InTalent and Prog. Atracción Talento, CM (Spain); SRC (Sweden); the Leverhulme Trust, the Royal Society and UKRI (United Kingdom).

References

- [1] CDF collaboration, F. Abe *et al.*, *Observation of the B_c meson in $p\bar{p}$ collisions at $\sqrt{s} = 1.8$ TeV*, Phys. Rev. Lett. **81** (1998) 2432, arXiv:hep-ex/9805034.
- [2] CDF collaboration, F. Abe *et al.*, *Observation of B_c mesons in $p\bar{p}$ collisions at $\sqrt{s} = 1.8$ TeV*, Phys. Rev. **D58** (1998) 112004, arXiv:hep-ex/9804014.
- [3] LHCb collaboration, R. Aaij *et al.*, *Measurement of $\sigma(pp \rightarrow b\bar{b}X)$ at $\sqrt{s} = 7$ TeV in the forward region*, Phys. Lett. **B694** (2010) 209, arXiv:1009.2731.
- [4] LHCb collaboration, R. Aaij *et al.*, *Measurement of J/ψ production in pp collisions at $\sqrt{s} = 7$ TeV*, Eur. Phys. J. **C71** (2011) 1645, arXiv:1103.0423.
- [5] LHCb collaboration, R. Aaij *et al.*, *Measurement of the B^\pm production cross-section in pp collisions at $\sqrt{s} = 7$ TeV*, JHEP **04** (2012) 093, arXiv:1202.4812.
- [6] LHCb collaboration, R. Aaij *et al.*, *Measurement of B meson production cross-sections in proton-proton collisions at $\sqrt{s} = 7$ TeV*, JHEP **08** (2013) 117, arXiv:1306.3663.
- [7] LHCb collaboration, R. Aaij *et al.*, *Production of J/ψ and Υ mesons in pp collisions at $\sqrt{s} = 8$ TeV*, JHEP **06** (2013) 064, arXiv:1304.6977.
- [8] LHCb collaboration, R. Aaij *et al.*, *Measurement of forward J/ψ production cross-sections in pp collisions at $\sqrt{s} = 13$ TeV*, JHEP **10** (2015) 172, Erratum *ibid.* **05** (2017) 063, arXiv:1509.00771.
- [9] LHCb collaboration, R. Aaij *et al.*, *First observation of the decay $B_c^+ \rightarrow J/\psi\pi^+\pi^-\pi^+$* , Phys. Rev. Lett. **108** (2012) 251802, arXiv:1204.0079.
- [10] LHCb collaboration, R. Aaij *et al.*, *Observation of the decay $B_c^+ \rightarrow \psi(2S)\pi^+$* , Phys. Rev. **D87** (2013) 071103(R), arXiv:1303.1737.
- [11] LHCb collaboration, R. Aaij *et al.*, *Observation of $B_c^+ \rightarrow J/\psi D_s^+$ and $B_c^+ \rightarrow J/\psi D_s^{*+}$ decays*, Phys. Rev. **D87** (2013) 112012, Erratum *ibid.* **D89** (2014) 019901(E), arXiv:1304.4530.
- [12] LHCb collaboration, R. Aaij *et al.*, *First observation of the decay $B_c^+ \rightarrow J/\psi K^+$* , JHEP **09** (2013) 075, arXiv:1306.6723.
- [13] LHCb collaboration, R. Aaij *et al.*, *Observation of the decay $B_c^+ \rightarrow B_s^0\pi^+$* , Phys. Rev. Lett. **111** (2013) 181801, arXiv:1308.4544.
- [14] LHCb collaboration, R. Aaij *et al.*, *Observation of the decay $B_c^+ \rightarrow J/\psi K^+K^-\pi^+$* , JHEP **11** (2013) 094, arXiv:1309.0587.
- [15] LHCb collaboration, R. Aaij *et al.*, *Evidence for the decay $B_c^+ \rightarrow J/\psi 3\pi^+2\pi^-$* , JHEP **05** (2014) 148, arXiv:1404.0287.
- [16] LHCb collaboration, R. Aaij *et al.*, *First observation of a baryonic B_c^+ decay*, Phys. Rev. Lett. **113** (2014) 152003, arXiv:1408.0971.

- [17] LHCb collaboration, R. Aaij *et al.*, *Measurement of B_c^+ production in proton-proton collisions at $\sqrt{s} = 8$ TeV*, Phys. Rev. Lett. **114** (2015) 132001, arXiv:1411.2943.
- [18] LHCb collaboration, R. Aaij *et al.*, *Measurement of the lifetime of the B_c^+ meson using the $B_c^+ \rightarrow J/\psi\pi^+$ decay mode*, Phys. Lett. **B742** (2015) 29, arXiv:1411.6899.
- [19] CMS collaboration, V. Khachatryan *et al.*, *Measurement of the ratio of the production cross sections times branching fractions of $B_c^\pm \rightarrow J/\psi\pi^\pm$ and $B^\pm \rightarrow J/\psi K^\pm$ and $\mathcal{B}(B_c^\pm \rightarrow J/\psi\pi^\pm\pi^\pm\pi^\mp)/\mathcal{B}(B_c^\pm \rightarrow J/\psi\pi^\pm)$ in pp collisions at $\sqrt{s} = 7$ TeV*, JHEP **01** (2015) 063, arXiv:1410.5729.
- [20] LHCb collaboration, R. Aaij *et al.*, *Measurement of the branching fraction ratio $\mathcal{B}(B_c^+ \rightarrow \psi(2S)\pi^+)/\mathcal{B}(B_c^+ \rightarrow J/\psi\pi^+)$* , Phys. Rev. **D92** (2015) 072007, arXiv:1507.03516.
- [21] ATLAS collaboration, G. Aad *et al.*, *Study of the $B_c^+ \rightarrow J/\psi D_s^+$ and $B_c^+ \rightarrow J/\psi D_s^{*+}$ decays with the ATLAS detector*, Eur. Phys. J. **C76** (2016) 4, arXiv:1507.07099.
- [22] LHCb collaboration, R. Aaij *et al.*, *Search for B_c^+ decays to the $p\bar{p}\pi^+$ final state*, Phys. Lett. **B759** (2016) 313, arXiv:1603.07037.
- [23] LHCb collaboration, R. Aaij *et al.*, *Study of B_c^+ decays to the $K^+K^-\pi^+$ final state and evidence for the decay $B_c^+ \rightarrow \chi_{c0}\pi^+$* , Phys. Rev. **D94** (2016) 091102(R), arXiv:1607.06134.
- [24] LHCb collaboration, R. Aaij *et al.*, *Measurement of the ratio of branching fractions $\mathcal{B}(B_c^+ \rightarrow J/\psi K^+)/\mathcal{B}(B_c^+ \rightarrow J/\psi\pi^+)$* , JHEP **09** (2016) 153, arXiv:1607.06823.
- [25] LHCb collaboration, R. Aaij *et al.*, *Observation of $B_c^+ \rightarrow J/\psi D^{(*)}K^{(*)}$ decays*, Phys. Rev. **D95** (2017) 032005, arXiv:1612.07421.
- [26] LHCb collaboration, R. Aaij *et al.*, *Observation of $B_c^+ \rightarrow D^0 K^+$ decays*, Phys. Rev. Lett. **118** (2017) 111803, arXiv:1701.01856.
- [27] LHCb collaboration, R. Aaij *et al.*, *Measurement of the ratio of branching fractions $\mathcal{B}(B_c^+ \rightarrow J/\psi\tau^+\nu_\tau)/\mathcal{B}(B_c^+ \rightarrow J/\psi\mu^+\nu_\mu)$* , Phys. Rev. Lett. **120** (2018) 121801, arXiv:1711.05623.
- [28] LHCb collaboration, R. Aaij *et al.*, *Search for B_c^+ decays to two charm mesons*, Nucl. Phys. **B930** (2018) 563, arXiv:1712.04702.
- [29] CMS collaboration, A. M. Sirunyan *et al.*, *Measurement of b hadron lifetimes in pp collisions at $\sqrt{s} = 8$ TeV*, Eur. Phys. J. **C78** (2018) 457, Erratum *ibid.* **C78** (2018) 561, arXiv:1710.08949.
- [30] CMS collaboration, A. M. Sirunyan *et al.*, *Observation of two excited B_c^+ states and measurement of the $B_c^+(2S)$ mass in pp collisions at $\sqrt{s} = 13$ TeV*, Phys. Rev. Lett. **122** (2019) 132001, arXiv:1902.00571.
- [31] LHCb collaboration, R. Aaij *et al.*, *Observation of an excited B_c^+ state*, Phys. Rev. Lett. **122** (2019) 232001, arXiv:1904.00081.

- [32] LHCb collaboration, R. Aaij *et al.*, *Measurement of the B_c^- meson production fraction and asymmetry in 7 and 13 TeV pp collisions*, Phys. Rev. **D100** (2019) 112006, arXiv:1910.13404.
- [33] LHCb collaboration, R. Aaij *et al.*, *Precision measurement of the B_c^+ meson mass*, JHEP **07** (2020) 123, arXiv:2004.08163.
- [34] LHCb collaboration, R. Aaij *et al.*, *Updated search for B_c^+ decays to two charm mesons*, JHEP **12** (2021) 117, arXiv:2109.00488.
- [35] LHCb collaboration, R. Aaij *et al.*, *Study of B_c^+ decays to charmonia and three light hadrons*, JHEP **01** (2022) 065, arXiv:2111.03001.
- [36] LHCb collaboration, R. Aaij *et al.*, *Study of B_c^+ meson decays to charmonia plus multihadron final states*, JHEP **07** (2023) 198, arXiv:2208.08660.
- [37] M. Bauer, B. Stech, and M. Wirbel, *Exclusive non-leptonic decays of D-, D_s^- , and B-mesons*, Z. Phys. **C34** (1987) 103.
- [38] M. Wirbel, *Description of weak decays of D and B mesons*, Prog. Part. Nucl. Phys. **21** (1988) 33.
- [39] S. S. Gershtein, V. V. Kiselev, A. K. Likhoded, and A. V. Tkabladze, *Physics of B_c -mesons*, Phys. Usp. **38** (1995) 1, arXiv:hep-ph/9504319.
- [40] S. S. Gershtein *et al.*, *Theoretical status of the B_c meson*, in *IV Workshop on Heavy Quark Physics*, 1997, arXiv:hep-ph/9803433.
- [41] V. V. Kiselev, A. K. Likhoded, and A. I. Onishchenko, *Semileptonic B_c -meson decays in sum rules of QCD and NRQCD*, Nucl. Phys. **B569** (2000) 473, arXiv:hep-ph/9905359.
- [42] V. V. Kiselev, A. E. Kovalsky, and A. K. Likhoded, *B_c decays and lifetime in QCD sum rules*, Nucl. Phys. **B585** (2000) 353, arXiv:hep-ph/0002127.
- [43] D. Ebert, R. N. Faustov, and V. O. Galkin, *Properties of heavy quarkonia and B_c mesons in the relativistic quark model*, Phys. Rev. **D67** (2003) 014027, arXiv:hep-ph/0210381.
- [44] A. K. Likhoded and A. V. Luchinsky, *Light hadron production in $B_c \rightarrow J/\psi + X$ decays*, Phys. Rev. **D81** (2010) 014015, arXiv:0910.3089.
- [45] A. K. Likhoded and A. V. Luchinsky, *Production of a pion system in exclusive $B_c \rightarrow V(P) + n\pi$ decays*, Phys. Atom. Nucl. **76** (2013) 787.
- [46] A. V. Berezhnoy, A. K. Likhoded, and A. V. Luchinsky, *$B_c \rightarrow J/\psi(B_s, B_s^*) + n\pi$ decays*, PoS **QFTHEP2011** (2012) 076, arXiv:1111.5952.
- [47] ARGUS collaboration, H. Albrecht *et al.*, *First evidence of χ_c production in B meson decays*, Phys. Lett. **B277** (1992) 209.
- [48] CLEO collaboration, M. S. Alam *et al.*, *Exclusive hadronic B decays to charm and charmonium final states*, Phys. Rev. **D50** (1994) 43, arXiv:hep-ph/9403295.

- [49] CLEO collaboration, P. Avery *et al.*, *Study of exclusive two-body B^0 meson decays to charmonium*, Phys. Rev. **D62** (2000) 051101(R), [arXiv:hep-ex/0004032](#).
- [50] BaBar collaboration, B. Aubert *et al.*, *Measurement of branching fractions for exclusive B decays to charmonium final states*, Phys. Rev. **D65** (2002) 032001, [arXiv:hep-ex/0107025](#).
- [51] BaBar collaboration, B. Aubert *et al.*, *Measurement of branching fractions and charge asymmetries for exclusive B decays to charmonium*, Phys. Rev. Lett. **94** (2005) 141801, [arXiv:hep-ex/0412062](#).
- [52] BaBar collaboration, B. Aubert *et al.*, *Search for factorization-suppressed $B \rightarrow \chi_c K^{(*)}$ decays*, Phys. Rev. Lett. **94** (2005) 171801, [arXiv:hep-ex/0501061](#).
- [53] BaBar collaboration, B. Aubert *et al.*, *Measurements of the absolute branching fractions of $B^\pm \rightarrow K^\pm X_{c\bar{c}}$* , Phys. Rev. Lett. **96** (2006) 052002, [arXiv:hep-ex/0510070](#).
- [54] BaBar collaboration, B. Aubert *et al.*, *Search for $B^+ \rightarrow X(3872)K^+$, $X(3872) \rightarrow J/\psi\gamma$* , Phys. Rev. **D74** (2006) 071101(R), [arXiv:hep-ex/0607050](#).
- [55] BaBar collaboration, B. Aubert *et al.*, *Evidence for $X(3872) \rightarrow \psi(2S)\gamma$ in $B^\pm \rightarrow X(3872)K^\pm$ decays and a study of $B \rightarrow c\bar{c}\gamma K$* , Phys. Rev. Lett. **102** (2009) 132001, [arXiv:0809.0042](#).
- [56] BaBar collaboration, J. P. Lees *et al.*, *Measurements of the absolute branching fractions of $B^\pm \rightarrow K^\pm X_{c\bar{c}}$* , Phys. Rev. Lett. **124** (2020) 152001, [arXiv:1911.11740](#).
- [57] Belle collaboration, N. Soni *et al.*, *Measurement of branching fractions for $B \rightarrow \chi_{c1(2)}K(K^*)$ at Belle*, Phys. Lett. **B634** (2006) 155, [arXiv:hep-ex/0508032](#).
- [58] Belle collaboration, R. Kumar *et al.*, *Observation of $B^\pm \rightarrow \chi_{c1}\pi^\pm$ and search for direct CP violation*, Phys. Rev. **D74** (2006) 051103(R), [arXiv:hep-ex/0607008](#).
- [59] Belle collaboration, R. Mizuk *et al.*, *Observation of two resonancelike structures in the $\pi^+\chi_{c1}$ mass distribution in exclusive $\bar{B}^0 \rightarrow K^-\pi^+\chi_{c1}$ decays*, Phys. Rev. **D78** (2008) 072004, [arXiv:0806.4098](#).
- [60] Belle collaboration, V. Bhardwaj *et al.*, *Observation of $X(3872) \rightarrow J/\psi\gamma$ and search for $X(3872) \rightarrow \psi'\gamma$ in B decays*, Phys. Rev. Lett. **107** (2011) 091803, [arXiv:1105.0177](#).
- [61] Belle collaboration, V. Bhardwaj *et al.*, *Inclusive and exclusive measurements of B decays to χ_{c1} and χ_{c2} at Belle*, Phys. Rev. **D93** (2016) 052016, [arXiv:1512.02672](#).
- [62] Belle collaboration, Y. Kato *et al.*, *Measurements of the absolute branching fractions of $B^+ \rightarrow X_{c\bar{c}}K^+$ and $B^+ \rightarrow \bar{D}^{(*)0}\pi^+$ at Belle*, Phys. Rev. **D97** (2018) 012005, [arXiv:1709.06108](#).
- [63] Belle collaboration, K. Chilikin *et al.*, *Evidence for $B^+ \rightarrow h_c K^+$ and observation of $\eta_c(2S) \rightarrow p\bar{p}\pi^+\pi^-$* , Phys. Rev. **D100** (2019) 012001, [arXiv:1903.06414](#).

- [64] CDF collaboration, D. Acosta *et al.*, *Branching ratio measurements of exclusive B^+ decays to charmonium with the collider detector at Fermilab*, Phys. Rev. **D66** (2002) 052005.
- [65] LHCb collaboration, R. Aaij *et al.*, *Observation of $B_s^0 \rightarrow \chi_{c1} \phi$ decay and study of $B^0 \rightarrow \chi_{c1,2} K^{*0}$ decays*, Nucl. Phys. **B874** (2013) 663, arXiv:1305.6511.
- [66] LHCb collaboration, R. Aaij *et al.*, *Observation of the decays $\Lambda_b^0 \rightarrow \chi_{c1} p K^-$ and $\Lambda_b^0 \rightarrow \chi_{c2} p K^-$* , Phys. Rev. Lett. **119** (2017) 062001, arXiv:1704.07900.
- [67] LHCb collaboration, R. Aaij *et al.*, *Observation of the decay $\bar{B}_s^0 \rightarrow \chi_{c2} K^+ K^-$* , JHEP **08** (2018) 191, arXiv:1806.10576.
- [68] LHCb collaboration, R. Aaij *et al.*, *Observation of the decay $\Lambda_b^0 \rightarrow \chi_{c1} p \pi^-$* , JHEP **05** (2021) 095, arXiv:2103.04949.
- [69] M. Beneke and L. Vernazza, *$B \rightarrow \chi_{cJ} K$ decays revisited*, Nucl. Phys. **B811** (2009) 155, arXiv:0810.3575.
- [70] C.-H. Chang, Y.-Q. Chen, G.-L. Wang, and H.-S. Zong, *Decays of the meson B_c to a P-wave charmonium state χ_c or h_c* , Phys. Rev. **D65** (2001) 014017, arXiv:hep-ph/0103036.
- [71] D. Ebert, R. N. Faustov, and V. O. Galkin, *Semileptonic and nonleptonic decays of B_c mesons to orbitally excited heavy mesons in the relativistic quark model*, Phys. Rev. **D82** (2010) 034019, arXiv:1007.1369.
- [72] E. Hernández, J. Nieves, and J. M. Verde-Velasco, *Study of exclusive semileptonic and nonleptonic decays of B_c^- in a nonrelativistic quark model*, Phys. Rev. **D74** (2006) 074008, arXiv:hep-ph/0607150.
- [73] M. A. Ivanov, J. G. Körner, and P. Santorelli, *Exclusive semileptonic and nonleptonic decays of the B_c meson*, Phys. Rev. **D73** (2006) 054024, arXiv:hep-ph/0602050.
- [74] V. V. Kiselev, O. N. Pakhomova, and V. A. Saleev, *Two-particle decays of the B_c meson into charmonium states*, J. Phys. G: Nucl. Part. Phys. **28** (2002) 595, arXiv:hep-ph/0110180.
- [75] Z. Rui, *Probing the P-wave charmonium decays of B_c meson*, Phys. Rev. **D97** (2018) 033001, arXiv:1712.08928.
- [76] Z.-h. Wang, G.-L. Wang, and C.-H. Chang, *The B_c decays to a P-wave charmonium by the improved Bethe–Salpeter approach*, J. Phys. G: Nucl. Part. Phys. **39** (2011) 015009, arXiv:1107.0474.
- [77] R. Zhu, *Relativistic corrections to the form factors of B_c into P-wave orbitally excited charmonium*, Nucl. Phys. **B931** (2018) 359, arXiv:1710.07011.
- [78] C.-H. Chang, Y.-Q. Chen, G.-L. Wang, and H.-S. Zong, *Semileptonic decays of B_c meson to a P-wave charmonium state χ_c or h_c^** , Commun. Theor. Phys. **35** (2001) 395, arXiv:hep-ph/0102150.


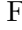
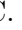








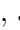

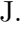

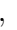
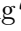



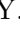
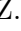




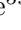


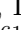

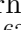




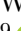
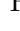

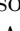
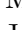
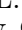




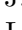
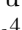





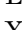





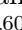










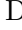

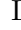


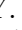
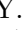




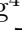
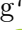



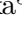
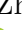
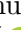

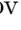






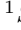
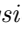
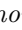
- [79] LHCb collaboration, A. A. Alves Jr. *et al.*, *The LHCb detector at the LHC*, JINST **3** (2008) S08005.
- [80] LHCb collaboration, R. Aaij *et al.*, *LHCb detector performance*, Int. J. Mod. Phys. **A30** (2015) 1530022, [arXiv:1412.6352](#).
- [81] R. Aaij *et al.*, *Performance of the LHCb Vertex Locator*, JINST **9** (2014) P09007, [arXiv:1405.7808](#).
- [82] R. Arink *et al.*, *Performance of the LHCb Outer Tracker*, JINST **9** (2014) P01002, [arXiv:1311.3893](#).
- [83] P. d'Argent *et al.*, *Improved performance of the LHCb Outer Tracker in LHC Run 2*, JINST **12** (2017) P11016, [arXiv:1708.00819](#).
- [84] LHCb collaboration, R. Aaij *et al.*, *Measurement of the Λ_b^0 , Ξ_b^- , and Ω_b^- baryon masses*, Phys. Rev. Lett. **110** (2013) 182001, [arXiv:1302.1072](#).
- [85] LHCb collaboration, R. Aaij *et al.*, *Precision measurement of D meson mass differences*, JHEP **06** (2013) 065, [arXiv:1304.6865](#).
- [86] E. E. Bowen, *Vertexing and tracking software at LHCb*, PoS **Vertex2014** (2014) 038.
- [87] A. Dziurda, *Studies of time dependent CP violation in charm decays of B_s^0 mesons*, PhD thesis, Institute of Nuclear Physics, Krakow, 2015, CERN-THESES-2015-246.
- [88] M. Adinolfi *et al.*, *Performance of the LHCb RICH detector at the LHC*, Eur. Phys. J. **C73** (2013) 2431, [arXiv:1211.6759](#).
- [89] A. A. Alves Jr. *et al.*, *Performance of the LHCb muon system*, JINST **8** (2013) P02022, [arXiv:1211.1346](#).
- [90] R. Aaij *et al.*, *The LHCb trigger and its performance in 2011*, JINST **8** (2013) P04022, [arXiv:1211.3055](#).
- [91] T. Sjöstrand, S. Mrenna, and P. Skands, *A brief introduction to PYTHIA 8.1*, Comput. Phys. Commun. **178** (2008) 852, [arXiv:0710.3820](#).
- [92] I. Belyaev *et al.*, *Handling of the generation of primary events in GAUSS, the LHCb simulation framework*, J. Phys. Conf. Ser. **331** (2011) 032047.
- [93] C.-H. Chang, C. Driouichi, P. Eerola, and X.-G. Wu, *BCVEGPy: an event generator for hadronic production of the B_c meson*, Comput. Phys. Commun. **159** (2004) 192, [arXiv:hep-ph/0309120](#).
- [94] C.-H. Chang, J.-X. Wang, and X.-G. Wu, *BCVEGPy 2.0: an upgraded version of the generator BCVEGPy with the addition of hadroproduction of the P-wave B_c states*, Comput. Phys. Commun. **174** (2006) 241, [arXiv:hep-ph/0504017](#).
- [95] X.-Y. Wang and X.-G. Wu, *A trick to improve the efficiency of generating unweighted B_c events from BCVEGPy*, Comput. Phys. Commun. **183** (2012) 442, [arXiv:1108.2442](#).

- [96] X.-G. Wu, BCVEGPY and GENXICC for the hadronic production of the doubly heavy mesons and baryons, J. Phys. Conf. Ser. **523** (2014) 012042, arXiv:1307.3344.
- [97] C.-H. Chang and Y.-Q. Chen, Hadronic production of the B_c meson at TeV energies, Phys. Rev. **D48** (1993) 4086.
- [98] C.-H. Chang, Y.-Q. Chen, G.-P. Han, and H.-T. Jiang, On hadronic production of the B_c meson, Phys. Lett. **B364** (1995) 78, arXiv:hep-ph/9408242.
- [99] C.-H. Chang, Y.-Q. Chen, and R. J. Oakes, Comparative study of the hadronic production of B_c mesons, Phys. Rev. **D54** (1996) 4344, arXiv:hep-ph/9602411.
- [100] K. Kołodziej, A. Leike, and R. Rückl, Production of B_c mesons in hadronic collisions, Phys. Lett. **B355** (1995) 337, arXiv:hep-ph/9505298.
- [101] A. V. Berezhnoy, V. V. Kiselev, and A. K. Likhoded, Hadronic production of S- and P-wave states of $\bar{b}c$ -quarkonium, Z. Phys. **A356** (1996) 79, arXiv:hep-ph/9602347.
- [102] D. J. Lange, The EVTGEN particle decay simulation package, Nucl. Instrum. Meth. **A462** (2001) 152.
- [103] N. Davidson, T. Przedzinski, and Z. Was, PHOTOS interface in C++ technical and physics documentation, Comput. Phys. Commun. **199** (2016) 86, arXiv:1011.0937.
- [104] Geant4 collaboration, J. Allison *et al.*, GEANT4 developments and applications, IEEE Trans. Nucl. Sci. **53** (2006) 270; Geant4 collaboration, S. Agostinelli *et al.*, GEANT4 – a simulation toolkit, Nucl. Instrum. Meth. **A506** (2003) 250.
- [105] M. Clemencic *et al.*, The LHCb simulation application, GAUSS: design, evolution and experience, J. Phys. Conf. Ser. **331** (2011) 032023.
- [106] R. Aaij *et al.*, Selection and processing of calibration samples to measure the particle identification performance of the LHCb experiment in Run 2, EPJ Tech. Instrum. **6** (2019) 1, arXiv:1803.00824.
- [107] LHCb collaboration, R. Aaij *et al.*, Measurement of the track reconstruction efficiency at LHCb, JINST **10** (2015) P02007, arXiv:1408.1251.
- [108] LHCb collaboration, R. Aaij *et al.*, Evidence for the decay $B^0 \rightarrow J/\psi\omega$ and measurement of the relative branching fractions of B_s^0 meson decays to $J/\psi\eta$ and $J/\psi\eta'$, Nucl. Phys. **B867** (2013) 547, arXiv:1210.2631.
- [109] LHCb collaboration, R. Aaij *et al.*, Observations of $B_s^0 \rightarrow \psi(2S)\eta$ and $B_{(s)}^0 \rightarrow \psi(2S)\pi^+\pi^-$ decays, Nucl. Phys. **B871** (2013) 403, arXiv:1302.6354.
- [110] E. Govorkova, Study of π^0/γ efficiency using B meson decays in the LHCb experiment, Phys. Atom. Nucl. **79** (2016) 1474, arXiv:1505.02960.
- [111] K. Govorkova, Study of photons and neutral pions reconstruction efficiency in the LHCb experiment, Master's thesis, Lomonosov Moscow State University, Moscow, Russia, 2015. CERN-THESIS-2015-272.

- [112] I. M. Belyaev, E. M. Govorkova, V. Y. Egorychev, and D. V. Savrina, *Study of π^0/γ reconstruction and selection efficiency in the LHCb experiment*, Moscow Univ. Phys. Bull. **70** (2015) 497.
- [113] L. Breiman, J. H. Friedman, R. A. Olshen, and C. J. Stone, *Classification and regression trees*, Wadsworth international group, Belmont, California, USA, 1984.
- [114] A. Powell *et al.*, *Particle identification at LHCb*, PoS **ICHEP2010** (2011) 020, LHCb-PROC-2011-008.
- [115] H. Terrier and I. Belyaev, *Particle identification with LHCb calorimeters*, LHCb-2003-092, 2003.
- [116] C. Abellán Beteta *et al.*, *Calibration and performance of the LHCb calorimeters in Run 1 and 2 at the LHC*, arXiv:2008.11556.
- [117] W. D. Hulsbergen, *Decay chain fitting with a Kalman filter*, Nucl. Instrum. Meth. **A552** (2005) 566, arXiv:physics/0503191.
- [118] Particle Data Group, R. L. Workman *et al.*, *Review of particle physics*, Prog. Theor. Exp. Phys. **2022** (2022) 083C01, and 2023 update.
- [119] S. Geisser, *Predictive inference: an introduction*, Chapman & Hall, New York, 1993.
- [120] G. Punzi, *Sensitivity of searches for new signals and its optimization*, eConf **C030908** (2003) MODT002, arXiv:physics/0308063.
- [121] LHCb collaboration, R. Aaij *et al.*, *Observation of J/ψ -pair production in pp collisions at $\sqrt{s} = 7$ TeV*, Phys. Lett. **B707** (2012) 52, arXiv:1109.0963.
- [122] T. Skwarnicki, *A study of the radiative cascade transitions between the Υ' and Υ resonances*, PhD thesis, Institute of Nuclear Physics, Krakow, 1986, DESY-F31-86-02.
- [123] BaBar collaboration, J. P. Lees *et al.*, *Branching fraction measurements of the color-suppressed decays \bar{B}^0 to $D^{(*)0}\pi^0$, $D^{(*)0}\eta$, $D^{(*)0}\omega$, and $D^{(*)0}\eta'$ and measurement of the polarization in the decay $\bar{B}^0 \rightarrow D^{*0}\omega$* , Phys. Rev. **D84** (2011) 112007, Erratum *ibid.* **87** (2013) 039901(E), arXiv:1107.5751.
- [124] E760 collaboration, T. A. Armstrong *et al.*, *Study of the χ_{c1} and χ_{c2} charmonium states formed in $\bar{p}p$ annihilations*, Nucl. Phys. **B373** (1992) 35.
- [125] E835 collaboration, M. Andreotti *et al.*, *Measurement of the resonance parameters of the $\chi_{c1}(1^3P_1)$ and $\chi_{c2}(1^3P_2)$ states of charmonium formed in $p\bar{p}$ annihilations*, Nucl. Phys. **B717** (2005) 34, arXiv:hep-ex/0503022.
- [126] LHCb collaboration, R. Aaij *et al.*, *χ_{c1} and χ_{c2} resonance parameters with the decays $\chi_{c1,c2} \rightarrow J/\psi\mu^+\mu^-$* , Phys. Rev. Lett. **119** (2017) 221801, arXiv:1709.04247.
- [127] S. Karlin and L. S. Shapley, *Geometry of moment spaces*, vol. 12 of *Memoirs of the American Mathematical Society*, American Mathematical Society, Providence, Rhode Island, 1953.

- [128] LHCb collaboration, R. Aaij *et al.*, *Observation of the $B_c^+ \rightarrow J/\psi\pi^+\pi^0$ decay*, arXiv:2402.05523, submitted to JHEP.
- [129] S. S. Wilks, *The large-sample distribution of the likelihood ratio for testing composite hypotheses*, Ann. Math. Stat. **9** (1938) 60.
- [130] A. L. Read, *Presentation of search results: The CL_s technique*, J. Phys. G: Nucl. Part. Phys. **28** (2002) 2693.
- [131] G. Cowan, K. Cranmer, E. Gross, and O. Vitells, *Asymptotic formulae for likelihood-based tests of new physics*, Eur. Phys. J. **C71** (2011) 1554, Erratum *ibid.* **C73** (2013) 2501, arXiv:1007.1727.
- [132] LHCb collaboration, *LHCb magnet: Technical Design Report*, CERN-LHCC-2000-007, 2000.
- [133] M. Pivk and F. R. Le Diberder, *sPlot: a statistical tool to unfold data distributions*, Nucl. Instrum. Meth. **A555** (2005) 356, arXiv:physics/0402083.
- [134] S. Jackman, *Bayesian analysis for the social sciences*, John Wiley & Sons, Inc., Hoboken, New Jersey, USA, 2009.
- [135] D. Martínez Santos and F. Dupertuis, *Mass distributions marginalized over per-event errors*, Nucl. Instrum. Meth. **A764** (2014) 150, arXiv:1312.5000.
- [136] LHCb collaboration, R. Aaij *et al.*, *Amplitude analysis of the $B^+ \rightarrow D^+D^-K^+$ decay*, Phys. Rev. **D102** (2020) 112003, arXiv:2009.00026.
- [137] A. Poluektov, *Kernel density estimation of a multidimensional efficiency profile*, JINST **10** (2015) P02011, arXiv:1411.5528.
- [138] LHCb collaboration, R. Aaij *et al.*, *Measurement of relative branching fractions of B decays to $\psi(2S)$ and J/ψ mesons*, Eur. Phys. J. **C72** (2012) 2118, arXiv:1205.0918.

F. De Vellis¹⁷, J.A. de Vries⁷⁶, F. Debernardis^{21,h}, D. Decamp¹⁰, V. Dedu¹²,
 L. Del Buono¹⁵, B. Delaney⁶², H.-P. Dembinski¹⁷, J. Deng⁸, V. Denysenko⁴⁸,
 O. Deschamps¹¹, F. Dettori^{29,k}, B. Dey⁷⁴, P. Di Nezza²⁵, I. Diachkov⁴¹,
 S. Didenko⁴¹, S. Ding⁶⁶, V. Dobishuk⁵⁰, A. D. Docheva⁵⁷, A. Dolmatov⁴¹,
 C. Dong⁴, A.M. Donohoe²⁰, F. Dordei²⁹, A.C. dos Reis², A. D. Dowling⁶⁶,
 A.G. Downes¹⁰, W. Duan⁶⁹, P. Duda⁷⁷, M.W. Dudek³⁸, L. Dufour⁴⁶, V. Duk³¹,
 P. Durante⁴⁶, M. M. Duras⁷⁷, J.M. Durham⁶⁵, O. D. Durmus⁷⁴, A. Dziurda³⁸,
 A. Dzyuba⁴¹, S. Easo⁵⁵, E. Eckstein⁷³, U. Egede¹, A. Egorychev⁴¹, V. Egorychev⁴¹,
 S. Eisenhardt⁵⁶, E. Ejopu⁶⁰, S. Ek-In⁴⁷, L. Eklund⁷⁹, M. Elashri⁶³,
 J. Ellbracht¹⁷, S. Ely⁵⁹, A. Ene⁴⁰, E. Epple⁶³, S. Escher¹⁶, J. Eschle⁴⁸,
 S. Esen¹⁹, T. Evans⁶⁰, F. Fabiano^{29,k,46}, L.N. Falcao², Y. Fan⁷, B. Fang^{71,13},
 L. Fantini^{31,r}, M. Faria⁴⁷, K. Farmer⁵⁶, D. Fazzini^{28,p}, L. Felkowski⁷⁷,
 M. Feng^{5,7}, M. Feo⁴⁶, M. Fernandez Gomez⁴⁴, A.D. Fernez⁶⁴, F. Ferrari²²,
 F. Ferreira Rodrigues³, S. Ferreres Sole³⁵, M. Ferrillo⁴⁸, M. Ferro-Luzzi⁴⁶,
 S. Filippov⁴¹, R.A. Fini²¹, M. Fiorini^{23,l}, K.M. Fischer⁶¹, D.S. Fitzgerald⁸⁰,
 C. Fitzpatrick⁶⁰, F. Fleuret¹⁴, M. Fontana²², L. F. Foreman⁶⁰, R. Forty⁴⁶,
 D. Foulds-Holt⁵³, M. Franco Sevilla⁶⁴, M. Frank⁴⁶, E. Franzoso^{23,l}, G. Frau¹⁹,
 C. Frei⁴⁶, D.A. Friday⁶⁰, J. Fu⁷, Q. Fuehring¹⁷, Y. Fujii¹, T. Fulghesu¹⁵,
 E. Gabriel³⁵, G. Galati^{21,h}, M.D. Galati³⁵, A. Gallas Torreira⁴⁴, D. Galli^{22,j},
 S. Gambetta⁵⁶, M. Gandelman³, P. Gandini²⁷, H. Gao⁷, R. Gao⁶¹, Y. Gao⁸,
 Y. Gao⁶, Y. Gao⁸, M. Garau^{29,k}, L.M. Garcia Martin⁴⁷, P. Garcia Moreno⁴³,
 J. García Pardiñas⁴⁶, K. G. Garg⁸, L. Garrido⁴³, C. Gaspar⁴⁶, R.E. Geertsema³⁵,
 L.L. Gerken¹⁷, E. Gersabeck⁶⁰, M. Gersabeck⁶⁰, T. Gershon⁵⁴,
 Z. Ghorbanimoghaddam⁵², L. Giambastiani³⁰, F. I. Giasemis^{15,e}, V. Gibson⁵³,
 H.K. Giemza³⁹, A.L. Gilman⁶¹, M. Giovannetti²⁵, A. Gioventù⁴³,
 P. Gironella Gironell⁴³, C. Giugliano^{23,l}, M.A. Giza³⁸, E.L. Gkougkousis⁵⁹,
 F.C. Glaser^{13,19}, V.V. Gligorov¹⁵, C. Göbel⁶⁷, E. Golobardes⁴², D. Golubkov⁴¹,
 A. Golutvin^{59,41,46}, A. Gomes^{2,a,†}, S. Gomez Fernandez⁴³, F. Goncalves Abrantes⁶¹,
 M. Goncerz³⁸, G. Gong⁴, J. A. Gooding¹⁷, I.V. Gorelov⁴¹, C. Gotti²⁸,
 J.P. Grabowski⁷³, L.A. Granado Cardoso⁴⁶, E. Graugés⁴³, E. Graverini^{47,t},
 L. Gazette⁵⁴, G. Graziani⁴⁶, A. T. Grecu⁴⁰, L.M. Greeven³⁵, N.A. Grieser⁶³,
 L. Grillo⁵⁷, S. Gromov⁴¹, C. Gu¹⁴, M. Guarise²³, M. Guittiere¹³, V. Guliaeva⁴¹,
 P. A. Günther¹⁹, A.-K. Guseinov⁴⁷, E. Gushchin⁴¹, Y. Guz^{6,41,46}, T. Gys⁴⁶,
 K. Habermann⁷³, T. Hadavizadeh¹, C. Hadjivasiliou⁶⁴, G. Haefeli⁴⁷, C. Haen⁴⁶,
 J. Haimberger⁴⁶, M. Hajheidari⁴⁶, M.M. Halvorsen⁴⁶, P.M. Hamilton⁶⁴,
 J. Hammerich⁵⁸, Q. Han⁸, X. Han¹⁹, S. Hansmann-Menzemer¹⁹, L. Hao⁷,
 N. Harnew⁶¹, T. Harrison⁵⁸, M. Hartmann¹³, J. He^{7,c}, K. Heijhoff³⁵,
 F. Hemmer⁴⁶, C. Henderson⁶³, R.D.L. Henderson^{1,54}, A.M. Hennequin⁴⁶,
 K. Hennessy⁵⁸, L. Henry⁴⁷, J. Herd⁵⁹, J. Herdieckerhoff¹⁷, P. Herrero Gascon¹⁹,
 J. Heuel¹⁶, A. Hicheur³, G. Hijano Mendizabal⁴⁸, D. Hill⁴⁷, S.E. Hollitt¹⁷,
 J. Horswill⁶⁰, R. Hou⁸, Y. Hou¹⁰, N. Howarth⁵⁸, J. Hu¹⁹, J. Hu⁶⁹, W. Hu⁶,
 X. Hu⁴, W. Huang⁷, W. Hulsbergen³⁵, R.J. Hunter⁵⁴, M. Hushchyn⁴¹,
 D. Hutchcroft⁵⁸, D. Ilin⁴¹, P. Ilten⁶³, A. Inglessi⁴¹, A. Iniukhin⁴¹, A. Ishteev⁴¹,
 K. Ivshin⁴¹, R. Jacobsson⁴⁶, H. Jage¹⁶, S.J. Jaimes Elles^{45,72}, S. Jakobsen⁴⁶,
 E. Jans³⁵, B.K. Jashal⁴⁵, A. Jawahery^{64,46}, V. Jevtic¹⁷, E. Jiang⁶⁴, X. Jiang^{5,7},
 Y. Jiang⁷, Y. J. Jiang⁶, M. John⁶¹, D. Johnson⁵¹, C.R. Jones⁵³, T.P. Jones⁵⁴,
 S. Joshi³⁹, B. Jost⁴⁶, N. Jurik⁴⁶, I. Juszczak³⁸, D. Kaminaris⁴⁷, S. Kandybei⁴⁹,
 Y. Kang⁴, M. Karacson⁴⁶, D. Karpenkov⁴¹, M. Karpov⁴¹, A. M. Kauniskangas⁴⁷,
 J.W. Kautz⁶³, F. Keizer⁴⁶, D.M. Keller⁶⁶, M. Kenzie⁵³, T. Ketel³⁵, B. Khanji⁶⁶,
 A. Kharisova⁴¹, S. Kholodenko³², G. Khreich¹³, T. Kirn¹⁶, V.S. Kirsebom²⁸,

P. Vincent¹⁵ , F.C. Volle¹³ , D. vom Bruch¹² , V. Vorobyev⁴¹, N. Voropaev⁴¹ ,
K. Vos⁷⁶ , G. Vouters¹⁰, C. Vrahas⁵⁶ , J. Walsh³² , E.J. Walton¹ , G. Wan⁶ ,
C. Wang¹⁹ , G. Wang⁸ , J. Wang⁶ , J. Wang⁵ , J. Wang⁴ , J. Wang⁷¹ , M. Wang²⁷ ,
N. W. Wang⁷ , R. Wang⁵² , X. Wang⁶⁹ , X. W. Wang⁵⁹ , Y. Wang⁸ , Z. Wang¹³ ,
Z. Wang⁴ , Z. Wang⁷ , J.A. Ward^{54,1} , M. Waterlaet⁴⁶, N.K. Watson⁵¹ ,
D. Websdale⁵⁹ , Y. Wei⁶ , B.D.C. Westhenry⁵² , D.J. White⁶⁰ , M. Whitehead⁵⁷ ,
A.R. Wiederhold⁵⁴ , D. Wiedner¹⁷ , G. Wilkinson⁶¹ , M.K. Wilkinson⁶³ ,
M. Williams⁶² , M.R.J. Williams⁵⁶ , R. Williams⁵³ , F.F. Wilson⁵⁵ , W. Wislicki³⁹ ,
M. Witek³⁸ , L. Witola¹⁹ , C.P. Wong⁶⁵ , G. Wormser¹³ , S.A. Wotton⁵³ , H. Wu⁶⁶ ,
J. Wu⁸ , Y. Wu⁶ , K. Wyllie⁴⁶ , S. Xian⁶⁹, Z. Xiang⁵ , Y. Xie⁸ , A. Xu³² , J. Xu⁷ ,
L. Xu⁴ , L. Xu⁴ , M. Xu⁵⁴ , Z. Xu¹¹ , Z. Xu⁷ , Z. Xu⁵ , D. Yang⁴ , S. Yang⁷ ,
X. Yang⁶ , Y. Yang^{26,n} , Z. Yang⁶ , Z. Yang⁶⁴ , V. Yeroshenko¹³ , H. Yeung⁶⁰ ,
H. Yin⁸ , C. Y. Yu⁶ , J. Yu⁶⁸ , X. Yuan⁵ , E. Zaffaroni⁴⁷ , M. Zavertyaev¹⁸ ,
M. Zdybal³⁸ , M. Zeng⁴ , C. Zhang⁶ , D. Zhang⁸ , J. Zhang⁷ , L. Zhang⁴ ,
S. Zhang⁶⁸ , S. Zhang⁶ , Y. Zhang⁶ , Y. Z. Zhang⁴ , Y. Zhao¹⁹ , A. Zharkova⁴¹ ,
A. Zhelezov¹⁹ , X. Z. Zheng⁴ , Y. Zheng⁷ , T. Zhou⁶ , X. Zhou⁸ , Y. Zhou⁷ ,
V. Zhovkovska⁵⁴ , L. Z. Zhu⁷ , X. Zhu⁴ , X. Zhu⁸ , V. Zhukov^{16,41} , J. Zhuo⁴⁵ ,
Q. Zou^{5,7} , D. Zuliani³⁰ , G. Zunica⁴⁷ .

¹*School of Physics and Astronomy, Monash University, Melbourne, Australia*

²*Centro Brasileiro de Pesquisas Físicas (CBPF), Rio de Janeiro, Brazil*

³*Universidade Federal do Rio de Janeiro (UFRJ), Rio de Janeiro, Brazil*

⁴*Center for High Energy Physics, Tsinghua University, Beijing, China*

⁵*Institute Of High Energy Physics (IHEP), Beijing, China*

⁶*School of Physics State Key Laboratory of Nuclear Physics and Technology, Peking University, Beijing, China*

⁷*University of Chinese Academy of Sciences, Beijing, China*

⁸*Institute of Particle Physics, Central China Normal University, Wuhan, Hubei, China*

⁹*Consejo Nacional de Rectores (CONARE), San Jose, Costa Rica*

¹⁰*Université Savoie Mont Blanc, CNRS, IN2P3-LAPP, Annecy, France*

¹¹*Université Clermont Auvergne, CNRS/IN2P3, LPC, Clermont-Ferrand, France*

¹²*Aix Marseille Univ, CNRS/IN2P3, CPPM, Marseille, France*

¹³*Université Paris-Saclay, CNRS/IN2P3, IJCLab, Orsay, France*

¹⁴*Laboratoire Leprince-Ringuet, CNRS/IN2P3, Ecole Polytechnique, Institut Polytechnique de Paris, Palaiseau, France*

¹⁵*LPNHE, Sorbonne Université, Paris Diderot Sorbonne Paris Cité, CNRS/IN2P3, Paris, France*

¹⁶*I. Physikalisches Institut, RWTH Aachen University, Aachen, Germany*

¹⁷*Fakultät Physik, Technische Universität Dortmund, Dortmund, Germany*

¹⁸*Max-Planck-Institut für Kernphysik (MPIK), Heidelberg, Germany*

¹⁹*Physikalisches Institut, Ruprecht-Karls-Universität Heidelberg, Heidelberg, Germany*

²⁰*School of Physics, University College Dublin, Dublin, Ireland*

²¹*INFN Sezione di Bari, Bari, Italy*

²²*INFN Sezione di Bologna, Bologna, Italy*

²³*INFN Sezione di Ferrara, Ferrara, Italy*

²⁴*INFN Sezione di Firenze, Firenze, Italy*

²⁵*INFN Laboratori Nazionali di Frascati, Frascati, Italy*

²⁶*INFN Sezione di Genova, Genova, Italy*

²⁷*INFN Sezione di Milano, Milano, Italy*

²⁸*INFN Sezione di Milano-Bicocca, Milano, Italy*

²⁹*INFN Sezione di Cagliari, Monserrato, Italy*

³⁰*Università degli Studi di Padova, Università e INFN, Padova, Padova, Italy*

³¹*INFN Sezione di Perugia, Perugia, Italy*

³²*INFN Sezione di Pisa, Pisa, Italy*

³³*INFN Sezione di Roma La Sapienza, Roma, Italy*

- ³⁴ INFN Sezione di Roma Tor Vergata, Roma, Italy
- ³⁵ Nikhef National Institute for Subatomic Physics, Amsterdam, Netherlands
- ³⁶ Nikhef National Institute for Subatomic Physics and VU University Amsterdam, Amsterdam, Netherlands
- ³⁷ AGH - University of Science and Technology, Faculty of Physics and Applied Computer Science, Kraków, Poland
- ³⁸ Henryk Niewodniczanski Institute of Nuclear Physics Polish Academy of Sciences, Kraków, Poland
- ³⁹ National Center for Nuclear Research (NCBJ), Warsaw, Poland
- ⁴⁰ Horia Hulubei National Institute of Physics and Nuclear Engineering, Bucharest-Magurele, Romania
- ⁴¹ Affiliated with an institute covered by a cooperation agreement with CERN
- ⁴² DS4DS, La Salle, Universitat Ramon Llull, Barcelona, Spain
- ⁴³ ICCUB, Universitat de Barcelona, Barcelona, Spain
- ⁴⁴ Instituto Galego de Física de Altas Enerxías (IGFAE), Universidade de Santiago de Compostela, Santiago de Compostela, Spain
- ⁴⁵ Instituto de Física Corpuscular, Centro Mixto Universidad de Valencia - CSIC, Valencia, Spain
- ⁴⁶ European Organization for Nuclear Research (CERN), Geneva, Switzerland
- ⁴⁷ Institute of Physics, Ecole Polytechnique Fédérale de Lausanne (EPFL), Lausanne, Switzerland
- ⁴⁸ Physik-Institut, Universität Zürich, Zürich, Switzerland
- ⁴⁹ NSC Kharkiv Institute of Physics and Technology (NSC KIPT), Kharkiv, Ukraine
- ⁵⁰ Institute for Nuclear Research of the National Academy of Sciences (KINR), Kyiv, Ukraine
- ⁵¹ University of Birmingham, Birmingham, United Kingdom
- ⁵² H.H. Wills Physics Laboratory, University of Bristol, Bristol, United Kingdom
- ⁵³ Cavendish Laboratory, University of Cambridge, Cambridge, United Kingdom
- ⁵⁴ Department of Physics, University of Warwick, Coventry, United Kingdom
- ⁵⁵ STFC Rutherford Appleton Laboratory, Didcot, United Kingdom
- ⁵⁶ School of Physics and Astronomy, University of Edinburgh, Edinburgh, United Kingdom
- ⁵⁷ School of Physics and Astronomy, University of Glasgow, Glasgow, United Kingdom
- ⁵⁸ Oliver Lodge Laboratory, University of Liverpool, Liverpool, United Kingdom
- ⁵⁹ Imperial College London, London, United Kingdom
- ⁶⁰ Department of Physics and Astronomy, University of Manchester, Manchester, United Kingdom
- ⁶¹ Department of Physics, University of Oxford, Oxford, United Kingdom
- ⁶² Massachusetts Institute of Technology, Cambridge, MA, United States
- ⁶³ University of Cincinnati, Cincinnati, OH, United States
- ⁶⁴ University of Maryland, College Park, MD, United States
- ⁶⁵ Los Alamos National Laboratory (LANL), Los Alamos, NM, United States
- ⁶⁶ Syracuse University, Syracuse, NY, United States
- ⁶⁷ Pontifícia Universidade Católica do Rio de Janeiro (PUC-Rio), Rio de Janeiro, Brazil, associated to ³
- ⁶⁸ School of Physics and Electronics, Hunan University, Changsha City, China, associated to ⁸
- ⁶⁹ Guangdong Provincial Key Laboratory of Nuclear Science, Guangdong-Hong Kong Joint Laboratory of Quantum Matter, Institute of Quantum Matter, South China Normal University, Guangzhou, China, associated to ⁴
- ⁷⁰ Lanzhou University, Lanzhou, China, associated to ⁵
- ⁷¹ School of Physics and Technology, Wuhan University, Wuhan, China, associated to ⁴
- ⁷² Departamento de Física, Universidad Nacional de Colombia, Bogota, Colombia, associated to ¹⁵
- ⁷³ Universität Bonn - Helmholtz-Institut für Strahlen und Kernphysik, Bonn, Germany, associated to ¹⁹
- ⁷⁴ Eotvos Lorand University, Budapest, Hungary, associated to ⁴⁶
- ⁷⁵ Van Swinderen Institute, University of Groningen, Groningen, Netherlands, associated to ³⁵
- ⁷⁶ Universiteit Maastricht, Maastricht, Netherlands, associated to ³⁵
- ⁷⁷ Tadeusz Kosciuszko Cracow University of Technology, Cracow, Poland, associated to ³⁸
- ⁷⁸ Universidade da Coruña, A Coruna, Spain, associated to ⁴²
- ⁷⁹ Department of Physics and Astronomy, Uppsala University, Uppsala, Sweden, associated to ⁵⁷
- ⁸⁰ University of Michigan, Ann Arbor, MI, United States, associated to ⁶⁶
- ⁸¹ Departement de Physique Nucleaire (SPhN), Gif-Sur-Yvette, France

^a Universidade de Brasília, Brasília, Brazil

^b Centro Federal de Educação Tecnológica Celso Suckow da Fonseca, Rio De Janeiro, Brazil

^c Hangzhou Institute for Advanced Study, UCAS, Hangzhou, China

^d*School of Physics and Electronics, Henan University , Kaifeng, China*

^e*LIP6, Sorbonne Universite, Paris, France*

^f*Excellence Cluster ORIGINS, Munich, Germany*

^g*Universidad Nacional Autónoma de Honduras, Tegucigalpa, Honduras*

^h*Università di Bari, Bari, Italy*

ⁱ*Università degli studi di Bergamo, Bergamo, Italy*

^j*Università di Bologna, Bologna, Italy*

^k*Università di Cagliari, Cagliari, Italy*

^l*Università di Ferrara, Ferrara, Italy*

^m*Università di Firenze, Firenze, Italy*

ⁿ*Università di Genova, Genova, Italy*

^o*Università degli Studi di Milano, Milano, Italy*

^p*Università di Milano Bicocca, Milano, Italy*

^q*Università di Padova, Padova, Italy*

^r*Università di Perugia, Perugia, Italy*

^s*Scuola Normale Superiore, Pisa, Italy*

^t*Università di Pisa, Pisa, Italy*

^u*Università della Basilicata, Potenza, Italy*

^v*Università di Roma Tor Vergata, Roma, Italy*

^w*Università di Siena, Siena, Italy*

^x*Università di Urbino, Urbino, Italy*

^y*Universidad de Alcalá, Alcalá de Henares , Spain*

^z*Department of Physics/Division of Particle Physics, Lund, Sweden*

[†]*Deceased*